JGR Earth Surface

Correspondence to:
M. Słowik,
slowikgeo@poczta.onet.pl

Conditions to Preserve the Sedimentary Record of Channel Planforms in Temperate Rivers of the Northern Hemisphere

Marcin Słowik[1] , **József Dezső[2], János Kovács[3,4]** , **Mariusz Gałka[5], and György Sipos[6]**

[1]Adam Mickiewicz University, Institute of Geology, Geohazards Research Unit, Poznań, Poland, [2]Department of Environmental and Physical Geography, University of Pécs, Institute of Geography and Earth Sciences, Pécs, Hungary, [3]Department of Geology and Meteorology, University of Pécs, Pécs, Hungary, [4]University of Pécs, Szentágothai Research Centre, Environmental Analytical and Geoanalytical Research Group, Pécs, Hungary, [5]Department of Biogeography, Paleoecology and Nature Conservation, University of Lodz, Faculty of Biology and Environmental Protection, Lodz, Poland, [6]Department of Geoinformatics, Physical and Environmental Geography, University of Szeged, Szeged, Hungary

Abstract We aim to identify conditions that influence the preservation of a complete record of channel planforms in the topmost layer of floodplains, prior to the maintenance in the rock record. We have tested a hypothesis that a successive decrease of stream power and channel belt width are necessary to preserve the record of channel planforms in the topmost floodplain layer over 10^3 to 10^4-year time scales. A literature review was conducted for rivers of the temperate zone of the Northern Hemisphere. Stream power, valley, and channel belt widths, paleodischarges, sediment grain-size, and age of paleochannels were used to identify four groups of rivers with preservation potential ranging from tens of thousands years to annual time scales. The decrease in stream power followed by sustained low stream power, and successive decrease of channel belt width were identified in rivers preserving a 10^3 to 10^4-year record of channel planforms. River valleys with the record of at least two generations of paleochannels, and valley width/channel belt width ratios between 6 and 12, potentially preserve fluvial records over 10^3 to 10^4-year time scales. We analyzed unusually well-preserved records of channel planforms from the Obra and Sió Rivers (central Europe). A determination of trends in changes of stream power and channel belt widths based on an extensive set of geophysical, geological data, and sediment dating from earlier studies, confirmed the tested hypothesis. The proposed framework can be extended by fluvial records preserved by large, and coastal rivers, with the potential to include ancient fluvial records.

Plain Language Summary Sediments deposited by rivers are archives preserving memory of past events, such as floods or changes in the type of channel (e.g., from braided to meandering). The memory of some rivers reaches back to thousands of years whereas others contain the record of channel changes from the last few years. We aim to define what conditions influence these differences. We analyzed changes in past discharges, flow energy, and widths and age of channel belts preserved in valley floors, in rivers situated in the temperate zone of the Northern Hemisphere. We found that a decrease in flow energy followed by sustained low energy of the flow, and successive decrease of channel belt width, favor the preservation of past fluvial events over 10^3 to 10^4-year time scales. Rivers containing annual records are shaped by high flow energy, often eroding the record of past events. We analyzed unusually well-preserved sedimentary records from the middle Obra and Sió Rivers (central Europe). They contain traces of former river channels from the last 13,000 and 18,000 years, respectively. In both cases, the flow energy and channel belt width decreased in particular generations of former channels, and this confirms the findings from the other analyzed rivers.

1. Introduction

A sedimentary record of channel planforms preserved in alluvial sediments provides information about past climate changes. This is because dry and humid periods influence the magnitude of discharge, sediment load, channel width and depth, velocity, slope, and roughness (Leopold & Wolman, 1957). These interactions are recorded in fluvial sedimentary architecture. There are seven orders of elements constituting fluvial sedimentary architecture – from the single lamina, through bar surface, bars, nested channel cuts, channel fills and channel belts, to a nested valley (Miall, 1985). The record of channel belts includes information about the type of channel planform including records of past fluvial events that is, channel cutoffs, avulsions, the occurrence of floods, and changes in sedimentation style.

Before this sedimentary information is preserved in the rock record, alluvial sediments undergo eroding and reworking. The completeness of this record depends on the magnitude of erosional events (Allen, 1984; Bridge & Best, 1997), discharge regime (cf. Nicolas et al., 2016), inter-annual discharge variability (cf. Fielding et al., 2018), sediment supply causing the occurrence of aggradation and avulsions (cf. Blum & Törnqvist, 2000; Makaske, 2001; van de Lageweg et al., 2016), and the interactions between these factors and base-level changes (Blum & Törnqvist, 2000; Jervey, 1988; Shanley & McCabe, 1991). Paola et al. (2018) reported that identification of periods of stasis in fluvial records is important because of the potential to identify events missing in the fluvial sedimentary record. Durkin et al. (2018) noted that final preservation of a meandering channel belt requires aggradation, and occurrence of avulsions. Ganti et al. (2020) reported that bar deposits are relatively well preserved in avulsion-dominated systems due to slow lateral migration rates (Ganti et al., 2020). Despite these studies, it is not fully understood what sequence of changes in flow energy and sediment supply conditions results in the preservation of channel planforms in floodplain sediments prior to their preservation in the rock record.

The main objective of our study is to identify the conditions, the occurrence of which, and changes of which to a new state of flow and sediment transport, resulting in the preservation of a complete record of a channel planform, that can be identified in the topmost part of floodplains. We define the term "preservation potential" as the ability to preserve a channel planform in the floodplain surface, and its topmost layer. "Complete record" is defined as the sedimentary record of a channel planform maintaining basic features of its geometry (i.e., channel width, thickness, and section connecting at least two inflection points allowing for calculation of sinuosity) preserved in the topmost layer of a floodplain.

Our study aims to test the hypothesis that a successive decrease of specific stream power and channel belt width are necessary conditions to preserve the record of channel planforms in the topmost floodplain layer over 10^3 to 10^4 ky time scales. The hypothesis was tested using estimations of stream power, sinuosity and braiding indices for generations of paleochannels identified in the topmost floodplain record of rivers situated in the temperate zone of the Northern Hemisphere. We also studied relations between valley widths, channel belt widths, and the age of paleochannels preserved in the analyzed river floodplains. The data for the estimations originate from the literature review (Table 1), limited to valley-confined rivers. The rivers we analyzed are separated from sea coasts by mountain ranges and moraine uplands, so the influence of the backwater effect is not considered in the present review.

We propose a framework of rivers with preservation potentials varying from tens of thousands years to annual time scales. Four groups of rivers were identified. The obtained results are discussed with reference to identification of potential sites preserving fluvial sedimentary records over 10^3 to 10^4 ky time scale, extension of the proposed framework by examples of coastal and large rivers, and implications of our findings for ancient fluvial records.

In the second part of this study, we present a detailed analysis of changes in stream power, aggradation rates, and channel belt widths in unusually well-preserved alluvial fills of the Sió River valley (Transdanubia, southern Hungary), and middle Obra River valley (western Poland). They maintain the sedimentary record of river planforms from the Late Pleniglacial (a period between ∼30,000 and 14,700 cal. BP) and Late Glacial (∼14,700–11,700 cal. BP), respectively. Previous research conducted in these areas referred to the evolution of channel planforms in the Obra (Słowik, 2013, 2014, 2016a, 2016b, 2018; Słowik, Gałka & Marciniak 2020), and Sió Valleys (Słowik et al., 2021). We used ground-penetrating radar (GPR), grain-size, and sediment dating data collected during the earlier studies to estimate the width and thickness of channel fills, values of paleodischarges, stream power, and aggradation rates for identified generations of paleochannels. The goal was to use these data toward testing the hypothesis on a successive decrease of potential specific stream power, and channel belt width, on the preservation of the fluvial record over 10^3 to 10^4 ky time scales using an extensive set of geophysical, geological data, and sediment dating, collected during the earlier studies conducted at these sites.

2. Materials and Methods

2.1. Literature Review

A literature review was carried out to study time scales of the sedimentary record of channel planforms in rivers of the temperate zone of the Northern Hemisphere (Figure 1; Table 1). We collected data regarding valley and channel belt width, channel width, and depth, grain-size, valley slope, bankfull discharge, paleodischarge, and

Table 1
Channel Dimensions, Bankfull Palaeodischarge, Median Grain-Size, Potential Specific Stream Power, and Age of Former Channels of Selected Temperate Rivers of the Northern Hemisphere

Name of river course	Channel planform	Width (m)	Thickness (m)	Qbf (m³ s⁻¹)	Slope	D_{50} (m)	Channel belt width (m)	Valley width (m)	Valley width/ channel belt width ratio	Sinuosity and braiding index *-Number-based BI **-Length-based BI	Specific stream power (W m⁻²)	Age (cal. yr BP)	References
Low energy (0.5–20.0 W m−2) meandering and anabranching rivers with successive decreases of channel belt widths													
Middle Obra river (Poland)	Large-scale meanders	80	4	91	0.00012	0.0002597	1,400	10,000	7.14	1.86	1.34	13,339–13,086	Słowik, Gałka and Marciniak (2020)
Middle Obra River (Poland)	Large-scale meanders	70	4	107.9	0.00012	0.0002587	1,100	10,000	9.09	3.03	2.73	13,109–13,824	
Middle Obra River (Poland)	Crevasse channels	62	3.5	7.9	0.0008	N/A	310	10,000	32.25	2–4* 2.06**	1	4,407–4,153	
Middle Obra River (Poland)	Sinuous channels	40	2	N/A	0.0002	0.0001903	450	10,000	22.2	1.23	2.44	6,788–6,566	
Middle Obra River (Poland)	Sinuous channels	40	4	15.9	0.00026	0.000241	450	10,000	22.2	1.2	1.01	AD 1770	
Middle Obra River (Poland)	Sinuous channels	100	3	13.3	0.00026	0.0001478	450	10,000	22.2	1.27	0.34	2,849–2,753	
Middle Obra River (Poland)	Sinuous channels	20	2	16.2	0.00026	0.0001256	450	10,000	22.2	1.23	2.06	3,614–3,495	
Middle Obra River (Poland)	Anabranching	75	3	13.2	0.0002	0.0001663	400	10,000	25	2–4* 3.12**	0.34	10,709–10,159	Słowik (2013, 2014)
Middle Obra River (Poland)	Anabranching	60	2.5	6	0.0002	0.0001663	400	10,000	25	2–4* 3.12**	0.2	10,709–10,159	
Middle Obra River (Poland)	Anabranching	70	3	5.6	0.0002	0.000117	400	10,000	25	2–4* 3.12**	0.16	7,736–7,421	
Middle Obra River (Poland)	Anabranching	30	3	3.7	0.0002	0.000117	400	10,000	25	2–4* 3.12**	0.24	7,736–7,421	
Middle Obra River (Poland)	Anabranching	60	3	8.9	0.0002	0.000117	400	10,000	25	2–4* 3.12**	0.29	7,736–7,421	
Middle Obra River (Poland)	Anabranching	50	3.5	3	0.0002	0.0001797	400	10,000	25	2–4* 3.12**	0.12	5,661–5,071	

Table 1
Continued

Name of river course	Channel planform	Width (m)	Thickness (m)	Qbf (m³ s⁻¹)	Slope	D_{50} (m)	Channel belt width (m)	Valley width (m)	Valley width/channel belt width ratio	Sinuosity and braiding index *-Number-based BI **-Length-based BI	Specific stream power (W m⁻²)	Age (cal. yr BP)	References
Middle Obra River (Poland)	Anabranching	50	3	4.5	0.0002	0.0001797	400	10,000	25	2–4* 3.12**	0.18	5,661–5,071	
Middle Obra River (Poland)	Anabranching	50	4	3.4	0.0002	0.0001797	400	10,000	25	2–4* 3.12**	0.13	5,661–5,071	
Middle Obra River (Poland)	Anabranching	60	4	5.4	0.0002	0.0001797	400	10,000	25	2–4* 3.12**	0.18	5,661–5,071	Słowik et al. (2021)
Sió River (Hungary)	Large-scale meanders	200	5	254.8	0.0006	0.0000813	3,000	3,000	1	1.58	7.5	18,050 (OSL date)	
Sió River (Hungary)	Large-scale meanders	250	5	334.6	0.0006	0.000075	3,000	3,000	1	1.47	7.88	N/A	
Sió River (Hungary)	Anabranching	60	3.5	54.2	0.0004	0.0000582	1,600	3,000	1.87	2–3* 2.86**	3.54	12,981–12,712	
Sió River (Hungary)	Anabranching	75	5	53	0.0004	0.0000341	1,600	3,000	1.87	2–3* 2.86**	2.77	9,888–9,550	
Sió River (Hungary)	Anabranching	70	4	32	0.0004	0.0000507	1,900	3,000	1.58	2–3* 2.86**	1.79	11,605–11,234	
Sió River (Hungary)	Anabranching	65	3.5	30.6	0.0004	0.0000467	1,600	3,000	1.87	2–3* 2.86**	1.85	12,640 (OSL date)	
Sió River (Hungary)	Small-scale meanders	40	1.8	13.3	0.0003	0.0001528	380	3,000	7.89	2.75	0.97	1,940 BP (OSL date)	
Sió River (Hungary)	Small-scale meanders	18	3.5	26.9	0.0003	0.0001249	380	3,000	7.89	3.37	4.39	710 BP (OSL date)	
Sió River (Hungary)	Small-scale meanders	40	3	12.8	0.0003	0.0001157	370	3,000	8.11	2.44	0.94	1,025 BP (OSL date)	
Sió River (Hungary)	Small-scale meanders	25	3	13.8	0.0003	0.000062	370	3,000	8.11	2.44	1.62	1,173 BP (OSL date)	
Upper Vistula River (Poland)	Meandering	42	3.5	136	0.0001	0.000325	1,500	9,000	6	1.66	3.2	1,573–1,001	Starkel (1996), Kalicki (1991), Starkel (2001)

Table 1
Continued

Name of river course	Channel planform	Width (m)	Thickness (m)	Qbf (m³ s⁻¹)	Slope	D_{50} (m)	Channel belt width (m)	Valley width (m)	Valley width/ channel belt width ratio	Sinuosity and braiding index *-Number-based BI **-Length-based BI	Specific stream power (W m⁻²)	Age (cal. yr BP)	References
Upper Vistula River (Poland)	Meandering	58	3.5	60	0.0001	0.000325	1,500	9,000	6	2.68	1.4	6,175–5,593	
upper Vistula River (Poland)	meandering	50	3.5	60	0.0001	0.000325	1,500	9,000	6	1.64	1.2	6,405–5,936	
Upper Vistula River (Poland)	Meandering	70	3.5	334	0.0001	0.000325	1,500	9,000	6	3.4	4.7	7,581–7,022	
Upper Vistula River (Poland)	Meandering	40	3.5	38.7	0.0001	0.000325	1,500	9,000	6	1.21	0.9	8,855–8,367	
Upper Vistula River (Poland)	Meandering	30	2	65	0.0001	0.000325	3,500	9,000	2.57	2.21	2.1	9,287–8,430	
Upper Vistula River (Poland)	Meandering	160	6	1,611	0.0001	0.000325	3,500	9,000	2.57	3.75	9.9	11,608–10,795	
Upper Vistula River (Poland)	Meandering	120	6	1,519	0.0001	0.000325	3,500	9,000	2.57	1.4	12.4	13,223–12,757	
Prosna River (Poland)	Meandering	51	2.5	119.5	0.00082	0.0003	600	1,800	3	1.35	18.8	12,746–12,335	Rotnicki and Młynarczyk (1989), Rotnicki (1991)
Prosna River (Poland)	Meandering	44	2.4	90.7	0.00082	0.0003	600	1,800	3	1.4	16.6	11,075–10,230	
Prosna River (Poland)	Meandering	18.4	2.8	40	0.00082	0.0003	300	1,800	6	1.92	17.5	7,969–7,590	
Prosna River (Poland)	Meandering	17	3.3	18.6	0.00082	0.0003	300	1,800	6	2.32	8.8	6,173–5,299	
Prosna River (Poland)	Meandering	20	2	22.5	0.00082	0.0003	150	1,800	12	3	9	AD 1982	
Warta River (Poland)	Meandering	76.5	3.4	166.3	0.00018	0.000325	2,500	6,000	2.4	3.57	3.8	15,453–11,825	Gonera and Kozarski (1987)
Warta River (Poland)	Meandering	121	3.8	263.9	0.00018	0.0002	2,500	6,000	2.4	1.87	3.8	14,794–13,437	
Warta River (Poland)	Meandering	45	2.2	51.8	0.00018	0.00025	2,000	2,000	3	2.14	2	13,579–13,174	

Table 1
Continued

Name of river course	Channel platform	Width (m)	Thickness (m)	Qbf (m³ s⁻¹)	Slope	D_{50} (m)	Channel belt width (m)	Valley width (m)	Valley width/channel belt width ratio	Sinuosity and braiding index *-Number-based BI **-Length-based BI	Specific stream power (W m⁻²)	Age (cal. yr BP)	References
Warta River (Poland)	Meandering	52	1.8	51.7	0.00018	0.000325	2,500	6,000	2.4	1.75	1.7	13,165–12,480	Turkowska et al. (2004)
Warta River (Poland)	Meandering	68.4	3.5	179	0.00018	0.0002	480	6,000	12.5	2.25	4.6	2,739–2,361	
Warta River (Poland)	Anabranching	70	6.5	81	0.00018	0.0002	N/A	6,000	N/A	2–4* 2.31**	2	13,137–12,461	
Warta River (Poland)	Anabranching	17	2	13.8	0.00018	0.0002	N/A	6,000	N/A	2–3* 3.35**	1.4	5,854–5,145	
Tisza River (Hungary)	Large-scale meanders	2,000	12	900	0.00005	0.0000625	4,000	10,000	2.5	2.3	0.22	33,000 BP (OSL date)	Vandenberghe et al. (2018), Kasse et al. (2010)
Tisza River (Hungary)	Large-scale meanders	600	14	900	0.00015	0.000249	10,000	10,000	1	2.9	2.21	33,000 BP	
Tisza River (Hungary)	Large-scale meanders	400	8	600	0.00015	0.000249	8,000	10,000	1.25	1.72	2.21	15,600 BP	
Tisza River (Hungary)	Large-scale meanders	1,000	12	900	0.00015	0.000249	10,000	10,000	1	1.83	1.32	33,487–31,890	
Tisza River (Hungary)	Large-scale meanders	600	10	600	0.00015	0.000249	8,000	10,000	1.25	2.11	1.47	23,561–22,965	
Tisza River (Hungary)	Large-scale meanders	500	8	600	0.00015	0.000249	8,000	10,000	1.25	1.96	1.76	24,158–23,367	
Tisza River (Hungary)	Large-scale meanders	400	6	600	0.00015	0.000249	8,000	10,000	1.25	4.3	2.21	22,290–21,081	
Tisza River (Hungary)	Small-scale meanders	220	5	400	0.00015	0.000249	4,000	10,000	2.5	2.7	2.67	5,645–5,497	
Tisza River (Hungary)	Small-scale meanders	105	5	400	0.00015	0.000249	4,000	10,000	2.5	3.46	5.6	10,547–10,293	
Tisza River (Hungary)	Small-scale meanders	170	10	760	0.00015	0.000249	3,200	10,000	3.12	1.51	6.58	Modern	
Low and moderate energy (0.5–45.0 W m−2) meandering and anastomosing rivers with constant widths of channel belts and aggrading conditions													
Morava (the Czech Republic)	Anastomosing	25	2.2	119	0.00094	0.0003	500	2,000	4	3–4* 3.52**	43.9	3,060 BP (OSL)	Bábek et al. (2018)
Morava (the Czech Republic)	Anastomosing	35	3	119	0.00094	0.0003	500	2,000	4	3–4* 3.52**	31.3	8,017–7,734	

Table 1
Continued

Name of river course	Channel planform	Width (m)	Thickness (m)	Qbf (m³ s⁻¹)	Slope	D_{50} (m)	Channel belt width (m)	Valley width (m)	Valley width/channel belt width ratio	Sinuosity and braiding index *-Number-based BI **-Length-based BI	Specific stream power (W m⁻²)	Age (cal. yr BP)	References
Morava (the Czech Republic)	Anastomosing	35	2.6	119	0.00094	0.0003	500	2,000	4	3–4* 3.52**	31.3	1,284–1,176	Makaske et al. (2002), Makaske et al. (2017)
Morava (the Czech Republic)	Anastomosing	25	2.6	119	0.00094	0.0003	500	2,000	4	3–4* 3.52**	43.9	2,359–2,066	
Upper Columbia (Canada)	Anastomosing	15	2.5	220	0.00011	0.00016	1,800	1,800	1	3–4* 3.62**	16.5	649–507	
Upper Columbia (Canada)	Anastomosing	50	8	220	0.00011	0.00016	1,800	1,800	1	3–4* 3.62**	5	4,515–3,875	
Upper Columbia (Canada)	Anastomosing	20	8	220	0.00011	0.00016	1,800	1,800	1	3–4* 3.62**	12.4	3,145–2,352	
Upper Columbia (Canada)	Anastomosing	20	4	220	0.00011	0.00016	1,800	1,800	1	3–4* 3.62**	12.4	1,359–1,295	
Upper Columbia (Canada)	Anastomosing	20	4	220	0.00011	0.00016	1,800	1,800	1	3–5* 4.44**	12.4	1,058–796	
Upper Columbia (Canada)	Anastomosing	60	9	220	0.00011	0.00016	1,800	1,800	1	3–5* 4.44**	4.1	3,835–3,702	
Upper Columbia (Canada)	Anastomosing	30	1.5	220	0.00011	0.00016	1,800	1,800	1	3–5* 4.44**	8.2	680–554	
Upper Columbia (Canada)	Anastomosing	60	6	220	0.00011	0.00016	1,800	1,800	1	3–5* 4.44**	4.1	4,085–3,651	
Middle Narew (Poland)	Anastomosing	15	3	13	0.00016	0.0005	2,500	2,500	1	4–6* 5.96**	7	1,925–1,314	Gradziński et al. (2003), Gradziński et al. (2000): *based on the age on interchannel areas
Middle Narew (Poland)	Anastomosing	35	4	13	0.00016	0.0005	2,500	2,500	1	4–6* 5.96**	0.6	1,000–4,000 BP*	

Table 1
Continued

Name of river course	Channel planform	Width (m)	Thickness (m)	Qbf (m³ s⁻¹)	Slope	D_{50} (m)	Channel belt width (m)	Valley width (m)	Valley width/channel belt width ratio	Sinuosity and braiding index *-Number-based BI **-Length-based BI	Specific stream power (W m⁻²)	Age (cal. yr BP)	References
middle Narew (Poland)	anastomosing	10	2	13	0.000165	0.0005	2,500	2,500	1	4–6* 5.96**	10.5	modern channel	
Middle Narew (Poland)	Anastomosing	5	1.5	13	0.0002	0.0005	2,500	2,500	1	4–6* 5.96**	5.1	1,000–4,000 BP*	Słowik (2011), Słowik (2016a); ** based on the age of floodplain sediments
Lower Obra (Poland)	Meandering	30	2	8	0.0001	0.00023	250	250	1	2.45	0.3	1,000–7,000 BP**	
Lower Obra (Poland)	Meandering	15	1.3	8	0.0001	0.00023	250	250	1	2.45	0.5	1,000–7,000 BP**	
Lower Obra (Poland)	Meandering	40	3	8	0.0001	0.00023	320	320	1	2.45	0.2	1,000–7,000 BP**	
Lower Obra (Poland)	Meandering	35	2.8	8	0.0001	0.00023	320	320	1	2.48	0.2	1,000–7,000 BP**	
Lower Obra (Poland)	Meandering	20	1.5	8	0.0001	0.00023	300	300	1	2.48	0.4	1,000–7,000 BP**	
Lower Obra (Poland)	Meandering	30	2	8	0.0001	0.00023	300	300	1	2.48	0.3	1,000–7,000 BP**	
Lower Obra (Poland)	Meandering	25	1.8	8	0.0001	0.00023	250	500	2	1.79	0.3	1,000–7,000 BP**	
Lower Obra (Poland)	Meandering	45	3.5	8	0.0001	0.00023	220	600	2.72	1.79	0.2	1,000–7,000 BP**	
Koppány River (Hungary)	Meandering	70	3.5	41.7	0.00015	0.00006115	600	1,000	1.66	3.63	0.9	12,675–12,421	Słowik, Dezső, et al. (2020)
Koppány River (Hungary)	Meandering	50	4	32.8	0.00015	0.000006115	400	1,000	2.5	2.7	1	3,898–3,700	
Koppány River (Hungary)	Meandering	60	4	33.6	0.00015	0.00006115	400	1,000	2.5	1.32	0.8	3,898–3,700	
Kapos River (Hungary)	Meandering	70	3	23.5	0.00012	0.00006115	600	1,000	1.66	1.54	0.4	8,416–8,215	

Table 1
Continued

Name of river course	Channel planform	Width (m)	Thickness (m)	Qbf (m³ s⁻¹)	Slope	D_{50} (m)	Channel belt width (m)	Valley width (m)	Valley width/channel belt width ratio	Sinuosity and braiding index *-Number-based BI **-Length-based BI	Specific stream power (W m⁻²)	Age (cal. yr BP)	References
Kapos River (Hungary)	Meandering	50	4	21.7	0.00012	0.00006115	600	1,000	1.66	1.62	0.5	8,416–8,215	Candel et al. (2017), Candel et al. (2018), Menting and Meijles (2019)
Kapos River (Hungary)	Meandering	50	5.5	39.4	0.00012	0.00006115	450	1,000	2.22	7.59	0.9	11,134–10,734	
Overijsselse Vecht (the Netherlands)	Meandering	20	2.2	25.5	0.00014	0.00033	500	1,000	2	N/A	1.75	2,739–2,117	
Overijsselse Vecht (the Netherlands)	Meandering	40	2	32	0.00014	0.00033	1,000	1,000	1	2.37	1.75	1914 AD	
Drentsche Aa (the Netherlands)	Meandering	3	1	1.8	0.00052	0.000245	100	300	3	2.04	0.5	Modern channel	
Drentsche Aa (the Netherlands)	Meandering	15	1	1.8	0.00052	0.000245	100	300	3	1.5	0.5	Modern channel	
Drentsche Aa (the Netherlands)	Meandering	10	1	1.8	0.00052	0.000245	100	300	3	N/A	0.92	2,941–2,001	
Drentsche Aa (the Netherlands)	Meandering	4	1	1.8	0.00052	0.000245	100	300	3	N/A	2.29	7,305–7,310	
Moderate and high energy (30–170 W m−2) meandering and anabranching rivers with constant channel belt widths and intensive lateral migration													
Allier (France)	Meandering	58	2.5	300	0.00067	0.0045	1,300	2,500	1.92	1.7	33.9	AD 2002–2011	Blom (1997), Crosato and Saleh (2011)
Allier (France)	Meandering	130	2.5	800	0.0008	0.016	1,300	2,500	1.92	1.59	48.3	AD 2002–2011	
Bollin (England)	Meandering	15	1.5	26	0.003	0.026	250	300	1.2	3.16	51	AD 1840–2000	Hooke (1995), Hooke (2004), Luchi et al. (2010)
Bollin (England)	Meandering	20	2.5	38	0.003	0.035	250	300	1.2	1.48	55.9	AD 1840–2000	
Dane (England)	Meandering	20	1.5	30	0.002	0.002	300	500	1.66	1.81	29.4	AD 1840–2015	Hooke (2007), Feeney et al. (2020)
Wear (England)	Anabranching	50	0.8	124.5	0.007	0.065	150	250	1.66	2–3* 2.56**	171	AD 1945–2007	Entwistle et al. (2018)

Table 1
Continued

Name of river course	Channel planform	Width (m)	Thickness (m)	Qbf (m³ s⁻¹)	Slope	D_{50} (m)	Channel belt width (m)	Valley width (m)	Valley width/ channel belt width ratio	Sinuosity and braiding index *-Number-based BI **-Length-based BI	Specific stream power (W m⁻²)	Age (cal. yr BP)	References
Wear (England)	Anabranching	50	2.2	124.5	0.007	0.065	150	250	1.66	1–2* 1.7**	171	AD 1945–2007	Bertoldi et al. (2009), Bertoldi et al. (2010)
High-energy (60.0–700.0 W m-2) braided rivers with channel belts reworking the whole valley width													
Tagliamento (Italy)	Braided	100	2	200	0.004	0.04	800	1,200	1.5	2–5* 2.96**	78.5	AD 1999–2008	Bertoldi et al. (2009), Bertoldi et al. (2010)
Tagliamento (Italy)	Braided	100	2	1,700	0.004	0.04	800	1,200	1.5	2–5* 2.96**	667.1	AD 1999–2008	
Kicking Horse (Canada)	Braided	12	4	240	0.002	0.064	400	400	1	2–5* 3.47**	392.4	AD 2004–2012	Cyples (2019), Cyples et al. (2020)
Kicking Horse (Canada)	Braided	25	4	320	0.002	0.064	400	400	1	2–5* 3.47**	251.1	AD 2004–2012	
South Saskatchewan (Canada)*	Braided	70	4	230	0.0003	0.0003	700	700	1	2–4* 2.94**	9.6	AD 2000–2004	Ashworth et al. (2011): * - valley section near Outlook
South Saskatchewan (Canada)*	Braided	100	4	595	0.0003	0.0003	700	700	1	2–4* 2.94**	116.7	AD 2000–2004	
South Saskatchewan (Canada)*	Braided	50	4	230	0.0003	0.0003	700	700	1	2–4* 2.94**	13.5	2000–2004	
Sagavanirktok (USA)	Braided	125	3.5	600	0.00135	0.0046	2,400	2,400	1	3–6* 4.69**	63.6	AD 1949–1985	Lunt et al. (2004)
Sagavarniktok (USA)	Braided	200	3.9	600	0.00135	0.0046	2,400	2,400	1	3–6* 4.69**	39.7	AD 1949–1985	
Sagavarniktok (USA)	Braided	40	1	600	0.00135	0.0046	2,400	2,400	1	3–6* 4.69**	198.6	AD 1949–1985	
Sagavarniktok (USA)	Braided	80	1	600	0.00135	0.0046	2,400	2,400	1	3–6* 4.69**	99.3	AD 1949–1985	
Sagavarniktok (USA)	Braided	120	2.2	600	0.00135	0.0046	2,400	2,400	1	3–6* 4.69**	66.2	AD 1949–1985	

1 - Sagavarniktok, 2 - upper Columbia, 3 - Kicking Horse, 4 - South Saskatchewan, 5 - upper Vistula, 6 - Prosna, 7 - Warta, 8 - Tisza, 9 - Morava,10 - Narew, 11 - Obra, 12 - Sió, 13 - Kapos and Koppany, 14 - Overijsselse Vecht, 15 - Drentsche Aa, 16 - Allier, 17 -Bollin, 18 - Dane, 19 - Wear, 20 - Tagliamento
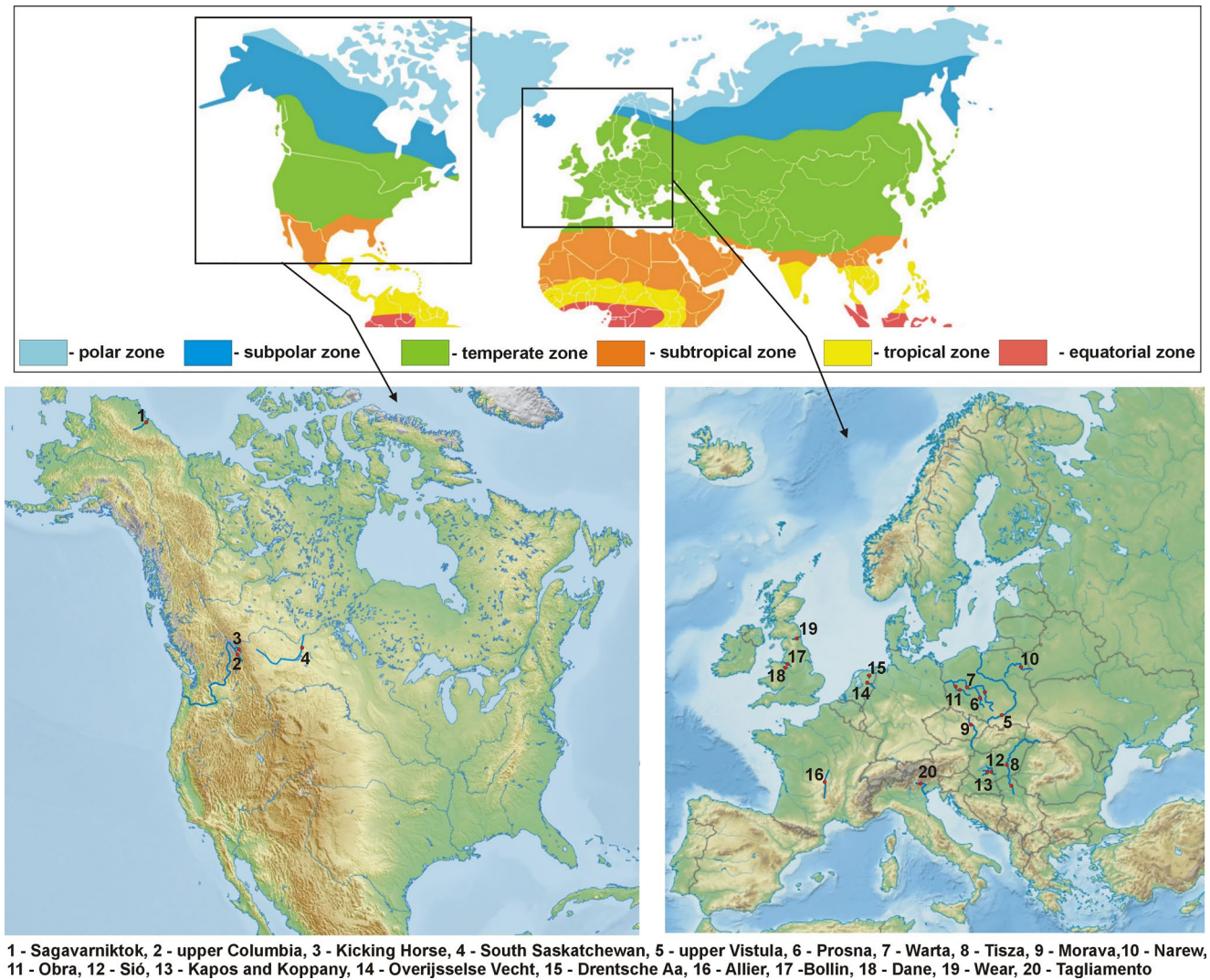
Figure 1. World's climate zones, and situation of rivers selected for review to study changes in stream power and a channel belt width of past channel planforms.

age of paleochannels. Where not available, widths of channels and channel belts were measured from topographic maps, aerial images, and geological sections, and Google Earth using the "distance measurement" tool. These data were used to estimate specific stream power for paleochannels preserved in the valley floors. The literature review was limited by the availability of the data, especially grain-size, aggradation rates, and reconstructions of channel planform changes. We have collected data from the following river valleys:

1. Rivers evolving in a postglacial landscape of central Europe: the Vistula (Wisła; Kalicki, 1991; Starkel et al., 1996; Starkel, 2001), Warta (Gonera & Kozarski, 1987), Prosna (Rotnicki, 1991; Rotnicki & Młynarczyk, 1989), middle Obra (Słowik, 2013, 2014; Słowik, Gałka & Marciniak, 2020) and lower Obra Valleys (Poland; Słowik, 2011, 2016a; 2016b).
2. Rivers of Transdanubia and Great Hungarian Plains (Hungary): the Kapos, Koppány (Słowik, Dezső, et al., 2020), Sió (Słowik et al., 2021), and Tisza River (Hungary; Kasse et al., 2010; Vandenberghe et al., 2018).
3. Low-energy rivers of western Europe: the Drentsche Aa and Overijssel Vecht (the Netherlands; Candel et al., 2017, 2018; Menting & Meijles, 2019).
4. Rivers evolving in valleys confined by mountain ranges or moraine uplands: the Morava (the Czech Republic; Bábek et al., 2018), upper Columbia (Canada) (Makaske et al., 2002, 2017), Narew (Poland; Gradziński et al., 2000, 2003).

5. Rivers characterized by active migration of meanders and formation of cutoffs: the Bollin and Dane Rivers (UK; Feeney et al., 2020; Hooke, 1995, 2004, 2007; Luchi et al., 2010); Allier River (France; Blom, 1997; Crosato & Saleh, 2011).

6. Anabranching rivers evolving in floodplains built of coarse sediments, and activating side channels at high flows: the Wear River (UK; Entwistle et al., 2018).

7. Braided rivers reworking their braidplains: the Tagliamento (Italy; Bertoldi et al., 2009, 2010), Kicking Horse (Canada; Cyples, 2019; Cyples et al., 2020), Sagavarniktok (northern slope of Alaska; Lunt et al., 2004), and South Saskatchewan River (Canada; Ashworth et al., 2011).

Sinuosity and braiding indices were determined for the channel planforms preserved in the valley floors of the selected rivers (Table 1). Sinuosity was calculated for meandering planforms by dividing the distance along paleochannels by a straight line distance between their upstream and downstream ends. Length-based braiding indices (BI_L) were determined for braided, and anabranching planforms by dividing the total length of channels in a valley section by the main channel length measured along the centerline of the channels (Mosley, 1981; in: Egozi & Ashmore, 2008; Friend & Sinha, 1993).

$$BI_L = \Sigma L_T / \Sigma L_M \tag{1}$$

where BI_L is the length-based braiding index, ΣL_T is the total length of channels, and ΣL_M is the length of the main channel.

Number-based braiding indices were calculated by counting the number of channels along valley cross-sections. As the number of channels varied between the cross-sections, a range of BI values was given in Table 1 for each of the analyzed rivers. The channel lengths were measured manually using maps and images found in the literature. When clear pictures of paleochannels preserved in valley floors were available in Google Earth, the measurements were carried out using the "distance measurement tool."

Sinuosity and braiding indices were calculated for channel belts preserved in the ancient rock record (Table S1). The aim was to compare geometry of channel planforms preserved in the surface layer of floodplains with the ancient record. An unpaired Welch *t*-test was performed to test the hypothesis that sinuosity of channel planforms from the Holocene and Late Glacial is not significantly different from sinuosity of the ancient channel belts (Table S2). The Welch's *t*-test was applied as the number of samples, standard deviation, and variances varied between the analyzed populations. The confidence interval was 95%. The test was run for sinuosity values.

Specific stream power was estimated for all the generations of paleochannels identified in the analyzed rivers (Table 1). Stream power describes the influence of flow energy to move the sediment from river banks and the bottom. This parameter shows how the changes in flow energy exert an influence on the type of channel planform (Ferguson, 1987; Kleinhans & van den Berg, 2011; van den Berg, 1995). Specific stream power (Bagnold, 1966) is defined as:

$$\omega = \rho g Q_{bf} S / w \tag{2}$$

where ω is potential specific stream power (W m^{-2}), ρ – density of water (g cm^{-3}), g – gravitation (m s^{-2}), Q_{bf} – bankfull discharge (m^3 s^{-1}), S – slope (m m^{-1}), w – bankfull channel width (m).

The uncertainties of bankfull paleodischarges, mean velocities and Manning's *n* coefficients were determined based on detailed field studies carried out in the Obra and Sió valleys, included in the conducted review (Tables 1, S3, and S4). This was done using an extensive set of geophysical and geological data collected during the earlier studies (Słowik, 2013, 2014, 2016a, 2016b, 2018; Słowik, Gałka & Marciniak, 2020; Słowik et al., 2021).

The estimated values of specific stream power were plotted with the median grain-size (D_{50}) of alluvial sediments on a graph delimiting types and channel planform and sediment load proposed by Kleinhans and van den Berg (2011). The goal was to compare the identified groups of rivers to types of planform and channel mobility estimated by Kleinhans and van den Berg (2011). The age of particular generations of the paleochannels was plotted with valley widths and valley width/channel belt width ratios. The aim was to verify how the observed changes in channel planforms are associated with the estimated trends in stream power and channel belt width.

3. Results of Literature Review – Conditions to Preserve the Sedimentary Record of Channel Planforms

We identified four groups of rivers characterized by preservation potentials ranging from tens of thousands years to annual time scales have been identified.

3.1. Low Energy (0.5–20.0 W m^{-2}) Meandering and Anabranching Rivers With a Successive Decrease of Channel Belt Widths

We have found that rivers preserving the record of channel planforms over 10^3 to 10^4 ky time scales are characterized by a decrease in potential specific stream power followed by sustained low stream power (Figure 2a1; Table 1). The decrease in stream power is accompanied by the increase in valley width/channel belt width ratio (Figure 2a2). This is because channel planforms of these rivers produce successively narrower channel belts. This group of rivers evolved from large-scale meanders to small-scale bends or anabranching channels in the Late Pleniglacial and Late Glacial. These transitions were accompanied by the increase in valley width/channel belt width ratios from 1–2 to 6–12 (Figure 2a2). Stream power decreased, and its low values were maintained in the early and middle Holocene until ∼4,000 cal. BP.

An increase in stream power can be seen in all the river courses during the last 4,000 years (Figure 2a1). This increase was small (e.g., from 0.5 to 1.0 W m^{-2} in the Warta River; Figure 2a1) and did not cause the erosion of the older channel fills. Valley width/channel belt width ratios turned from increasing to constant (Figure 2a2). The ability to preserve sequences of channel planforms by these rivers in a 10–20 ky time scale is confirmed by their locations in the diagram of Kleinhans and van den Berg (2011) (Figure 3). The middle Obra and Sió belong, as well as parts of the Warta, Vistula, and Tisza Rivers, to "laterally immobile" rivers. Large-scale meanders, and part of anabranching channels in the Sió Valley, and several channels in the Vistula, Prosna and Tisza Valleys belong to "moderately braided and meandering with scrolls and chutes", and "meandering with scrolls" (Figure 3). This means that the large-scale bends must have reworked the earlier fluvial record until being replaced by a lower energy planform.

3.2. Low and Moderate Energy (0.5–45.0 W m^{-2}) Meandering and Anastomosing Rivers With Constant Widths of Channel Belts and Aggrading Conditions

These rivers preserve traces of channel planforms reaching from 7,000 to 4,000 cal. yr BP (Figure 2b1). The Narew, upper Columbia, and Morava evolve through avulsions. Their valley width/channel belt width ratios amount to 1–3, and these values are constant in a millennial-scale. This is caused by constant widths of channel belts which rework the whole or at least half of the valley width (e.g., the lower Obra, Kapos and Koppány, upper Columbia and Narew; Figure 2b2). These rivers are confined by moraine uplands or mountain ranges and are characterized by periods of increased stream power (see Figure 2b1). This is why part of paleochannels preserved in the Narew, upper Columbia and Morava River valleys belong to meandering or moderately braided rivers in the diagram of Kleinhans and van den Berg (2011) (see Figure 3). Such a temporal increase in flow energy may have contributed to the formation of the avulsions, along with the influence of upstream sediment delivery (the upper Columbia River; Kleinhans et al., 2012; Makaske et al., 2017), and in-channel vegetation (Gradziński et al., 2003; Marcinkowski et al., 2018).

This group of rivers is characterized by aggrading conditions. Aggradation rates amounted to 1.77 mm y^{-1} during the last 4,550 cal. yr BP in the upper Columbia River (Makaske et al., 2002), 2.8 mm y^{-1} in the Morava River (Bábek et al., 2018) during the last ∼7,000 cal. yr BP, and 1.0–1.5 mm y^{-1} in the Narew River (Gradziński et al., 2003) during the last 4,000 cal. yr BP. The aggradation and relatively small valley width (compared to the previous group of rivers; Figure 4), led to the preservation of vertically stacked channel fills in these alluvial fills (multi-storey architecture of floodplains - cf. Gibling, 2006). Such an architecture also refers to rivers evolving through oblique aggradation (Drentsche Aa, the Netherlands; Candel et al., 2017). This process plays an important role in the preservation of channel bodies in the valley floor as the valley width is low (∼300 m; Figure 4) and limits the space for the preservation of channel planforms.

It should be noted that rivers evolving in valleys characterized by similar width (2.0–3.0 km) preserve channel planforms at a range of time scales, between 18,000 cal. yr BP and 4,000 cal. yr BP (see, e.g., the Prosna and
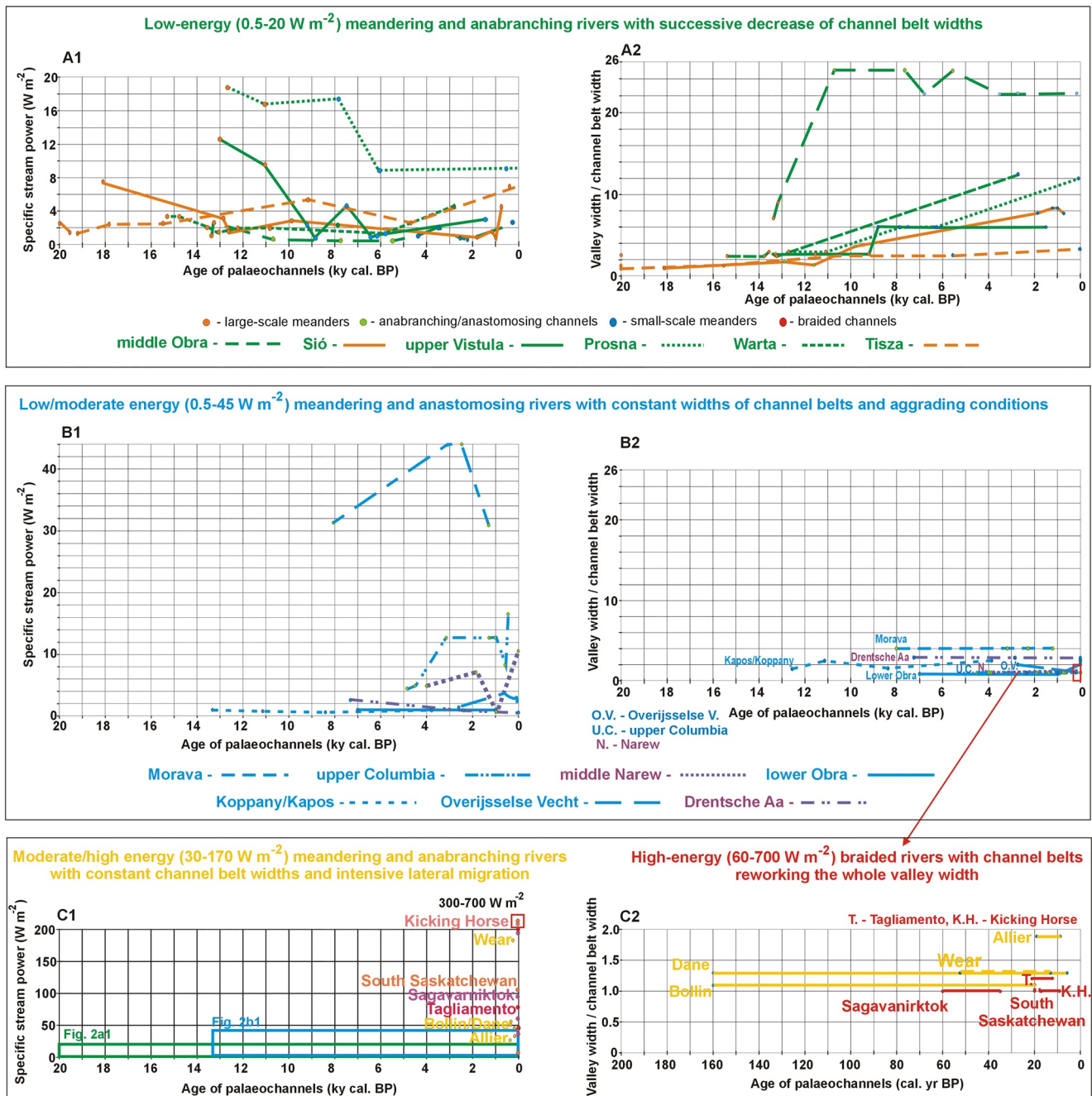
Figure 2. Types of rivers characterized by the preservation of channel planforms from millennial to annual time scales. The values of stream power, and valley width/channel belt width ratios were estimated for particular rivers, based on the values of paleodischarges, valley slopes, channel, and channel belt widths, and the age of paleochannels found in the literature (see Table 1 for data and references).

Warta, and the upper Columbia and Narew Rivers in Figure 4). Here the trends of changes in stream power, and valley width/channel belt width ratio discriminate between the record of channel planforms since the Late Glacial in the Prosna and Warta Valleys, and that since 5,000–4,000 cal. yr BP in the Columbia and Narew Valleys (Figures 2a and 2b).

Part of this group of rivers (Figure 2b1) are courses evolving through a slow migration of meanders, taking a millennial timescale to develop a meander bend. They preserve traces of meander migration from the last 8,000 years (the lower Obra Valley, Poland - Słowik, 2011) and paleomeanders from the last 13,500 years (Kapos
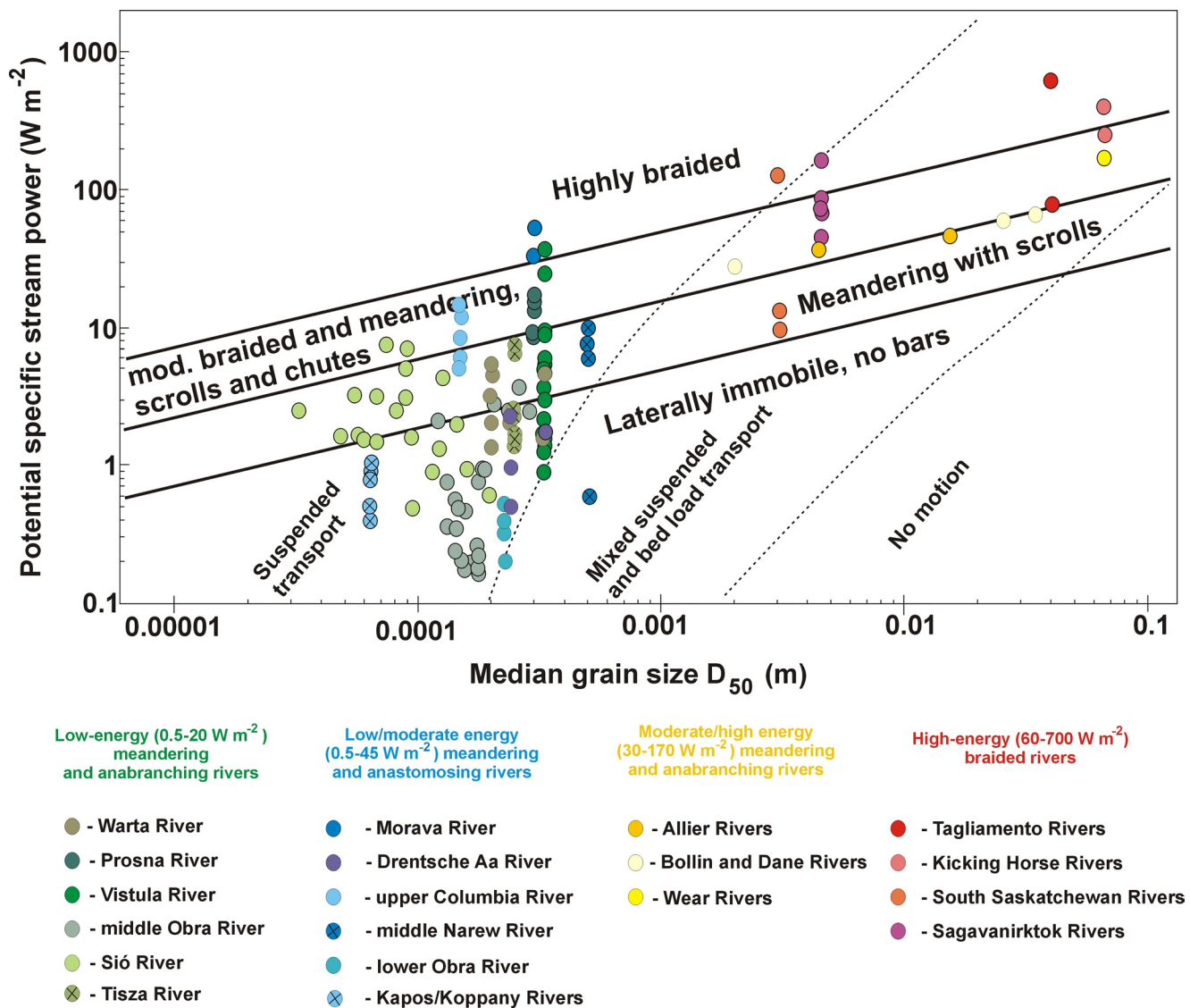
Figure 3. Specific stream power and median grain-size describing paleochannels preserved in identified groups of rivers.

and Koppány Valleys – Słowik, Dezső, et al., 2020). These rivers are featured with a constant low stream power not exceeding 1.0 W m^{-2} (Figure 2b1). They belong to "laterally immobile rivers" (cf. Kleinhans & van den Berg, 2011, Figure 3). Again, changes in channel belt width are important. For instance, the valley width/channel belt width ratio of the Sió Valley increases from 1.0 to 8.0 during the last 18,000 years. The ratio is close to constant (1.6–2.7) in the Kapos and Koppány Valleys over the period of 13,000 years. The Kapos and Koppány Valleys do not preserve the record of large-scale meanders from the Late Pleniglacial. High flows going through the Kapos and Koppány valleys formed braided channels at that time. Their traces are marked by layers of coarse sands in the valley bottom (cf. Lóczy & Dezső, 2013). The nature of these differences requires further studies.

3.3. Moderate and High Energy (30–170 W m^{-2}) Meandering and Anabranching Rivers With Constant Channel Belt Widths and Intensive Lateral Migration

These river valleys preserve the record of channel planform changes in centennial time scales. They are characterized by active migration of channels and occurrence of cutoffs. The channel belts of these rivers rework 75%–80% of their valley widths (valley width/channel belt width ratio amount to 1.2–1.7; Figure 2c2 and Table 1). They belong to meandering and moderately braided rivers on the diagram of Kleinhans and van den Berg (2011)
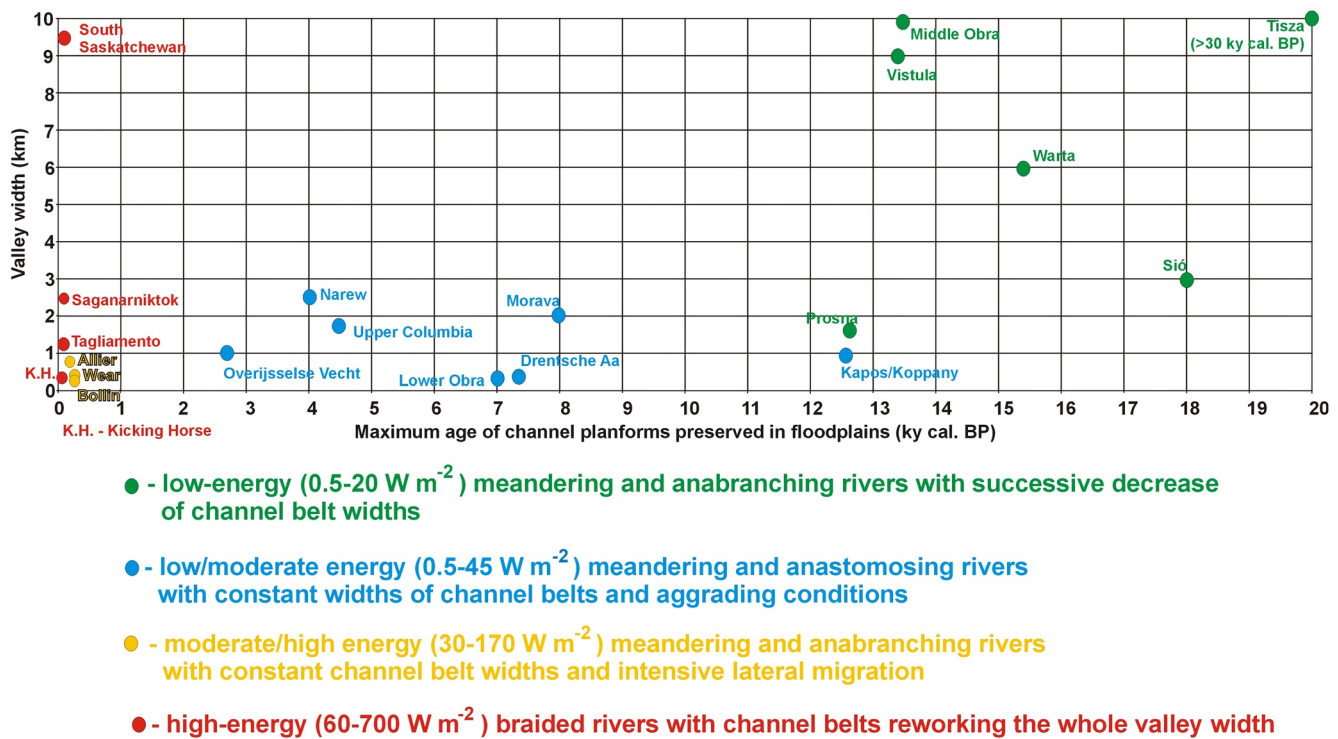
Figure 4. Valley widths and maximum age of channel planforms preserved in the alluvial sedimentary record. The valley widths were collected during the literature review or measured in aerial images using Google Earth.

(Figure 3). The sedimentary record of this type of river corresponds to the type of mobile channel belts (cf. Gibling, 2006, and see Figure 11b therein). The Allier (France), Bollin (the United Kingdom), and Wear River (the United Kingdom) represent these types of rivers. In the course of the Wear River, single-thread sections are characterized by increased bank erosion and reworking of the river bed (Entwistle et al., 2018). Thus, near the active channel belt, the scale of preservation can be decadal. Centennial sedimentary records may be preserved within terrace levels within incised sections of the valley. The Bollin and Dane Rivers (the United Kingdom) evolve through series of cutoffs (Hooke, 2004). As in the previous group of rivers, the width of channel belts is constant. However, these rivers migrate at a pace of 1.25–2.11 m y^{-1} (Hooke, 1995), and erode earlier fluvial records. Data shown by Hooke (2007; see Figure 2 therein) indicate that the planform of the Dane River from 1840 AD was reworked by later meander migration, and only single fragments of these meanders might be preserved in the alluvial deposits. The Allier River (France) is characterized by bend migration rates between 10.0 and 65.0 m y^{-1} (Crosato & Saleh, 2011). The intensive migration of meanders means that only single paleomeanders older than 1946 AD might be preserved in lateral parts of the valley (see Figure 1 of van Dijk et al., 2012).

3.4. High-Energy (60–700 W m^{-2}) Braided Rivers With Channel Belts Reworking the Whole Valley Width

These rivers represent the lowest ability to preserve past channel planforms owing to high stream power (Figure 2c1), and frequent eroding and reworking of the earlier fluvial record. The time scale of the preservation is annual to decadal. Valley width/channel belt width ratios amount to 1.0 (Figure 2c2; Table 1). This means that the channel belts of these rivers rework the whole width of these valleys. For instance, the course of the Tagliamento River (Italy) undergoes significant changes in channel width during intensive floods (cf. Bertoldi et al., 2009, 2010). The bankfull stage appears at least once per three years, and a complete reworking of the floodplain happens at least on a 10–20 year scale (Bertoldi et al., 2009). The channels of these rivers migrate rapidly; the average migration rate of the Kicking Horse River amounts from 9.0 to 34.0 m y^{-1}, and most of the valley floor can be reworked by high flows in a period of 8 years (see Figure 5 in Cyples et al., 2020). The channel belt of the Sagavanirktok River (north slope of Alaska) is reworked by flood flows occurring in the ice
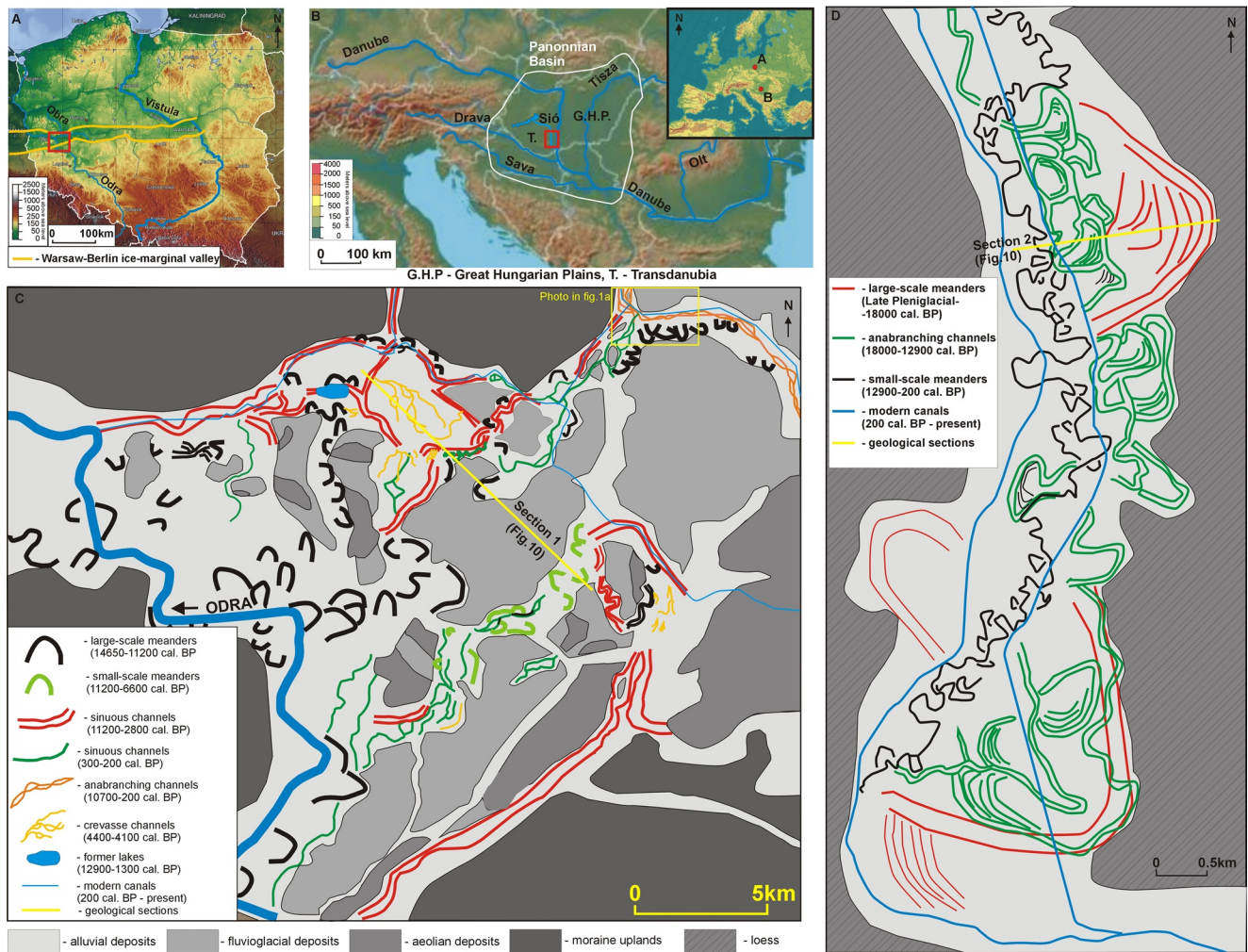
Figure 5. Geomorphic maps with the main types of channel planforms, and locations of the study sites. (a) Obra Valley (Poland), (b) Sió Valley (Hungary), (c) traces of a multi-channel connection between the Obra and Odra Rivers, with types of channel planforms identified by Słowik, Gałka and Marciniak (2020), (d) types of channel planforms preserved in the Sió Valley, identified by Słowik et al. (2021). The types of channel planforms distinguished in the maps originate from studies of Słowik, Gałka and Marciniak (2020 – the middle Obra Valley), and Słowik et al. (2021 – the Sió Valley). The main geological and geomorphological features were marked on the maps based on surface sediments geological maps (scale 1:50,000) edited by the Polish Geological Institute, and geological map of Hungary (scale 1:500,000) edited by the Mining and Geological Survey of Hungary.

breakup period in May and early June (Lunt et al., 2004). Braid bars change their shapes and locations by tens of meters in a 13-year period (see Figure 7 in Lunt et al., 2004). Despite dam construction, bed-load transport commences over the entire braidplain of the South Saskatchewan River (Canada) during flood events (Sambrook Smith et al., 2006). Its anabranches can be abandoned and filled with sediments within a 2-year period (Ashworth et al., 2011).

4. The Middle Obra and Sió Rivers – Examples of High Preservation Potential

We analyzed changes in specific stream power of former channels, widths of channel belts preserved in the valley floor, and aggradation rates in the middle Obra (Poland) and Sió River Valleys (Hungary). This was done in reference to a complex set of generations of paleochannels preserved in both valleys during the last 18,000 years (Figures 5–7). The middle Obra Valley is situated in a postglacial area, within the Warsaw-Berlin ice-marginal valley surrounded by moraine uplands (Figures 5a and 5c). The ice-marginal valley was formed by meltwater outwash of the Last Inland Ice (Marks, 2012). The surface area of the catchment measures 4,022 km². The width of the valley is ~10 km. The valley floor is filled with medium and fine sands, sandy silts, peats, and gyttjas.
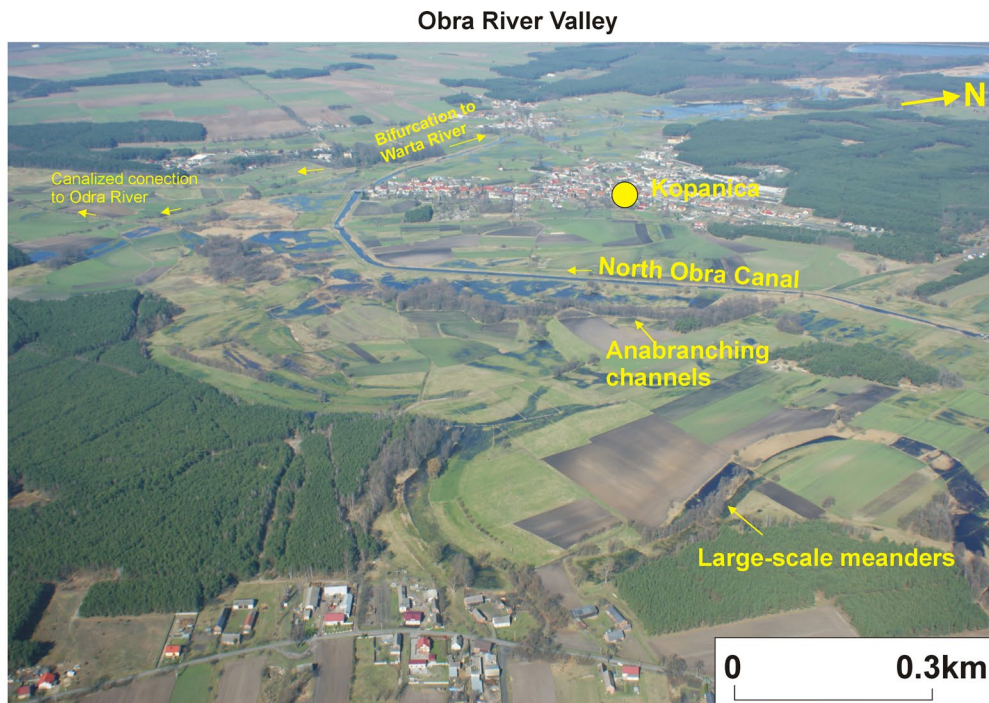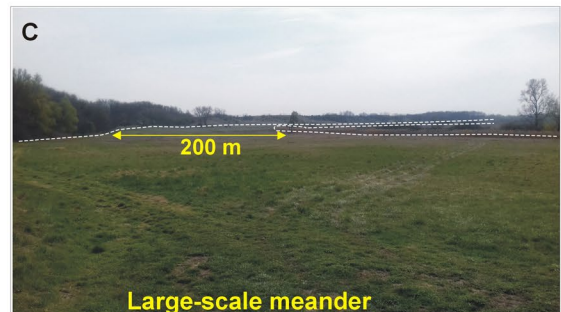
Figure 6. (a) Oblique aerial photograph (taken during an aerial survey on April1 2010) showing the main types of channel planforms preserved in the middle Obra River Valley, (b) aerial image of the Sió River Valley between Medina and Szedres (source: Google Earth). (c, d) Photographs showing traces and large-scale meanders and anabranching channels, respectively, in the Sió River Valley.

There are glacial (fragments of moraines) and aeolian (dunes and aeolian sands) landforms on the valley floor (Figure 5c). Alluvial sediments are present in 1–4 km wide "corridors", formed among the older landforms, marking locations of former channel belts (Figure 5c). In its western part, traces of a multi-channel connection with the Odra River are preserved in the valley floor (Słowik, Gałka & Marciniak, 2020). The middle Obra River formed large-scale meanders in the Late Glacial (Figures 6 and 7). The Sió valley is situated in Transdanubia
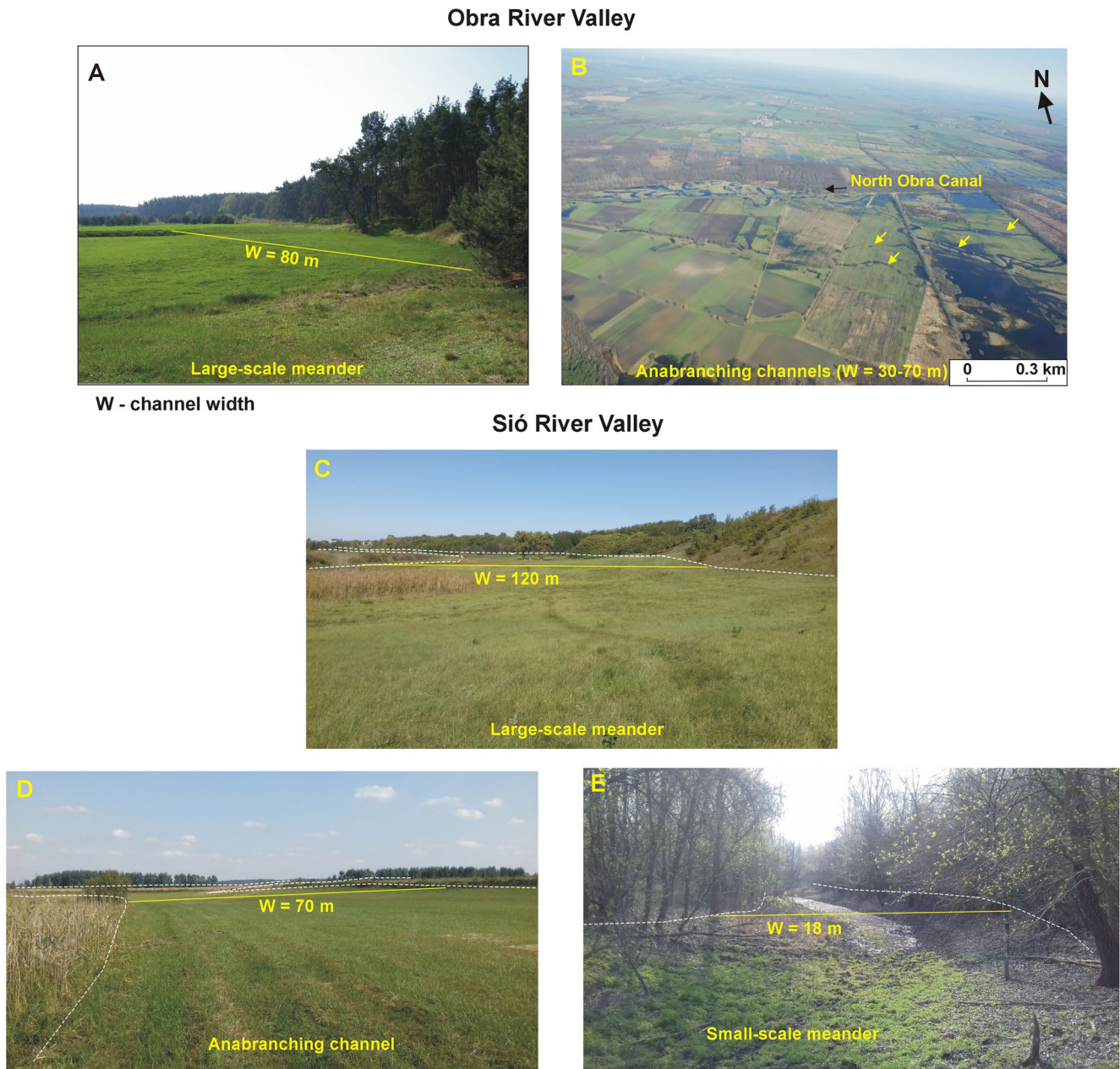
Figure 7. Photographs of paleochannels preserved in the middle Obra and Sió River Valleys: The middle Obra Valley: (a) large-scale meander, (b) oblique aerial photo (taken during an aerial survey on 1 April 2010) showing set of former anabranching channels. They are marked by yellow arrows. The survey was taken in a period of high water levels when the former channels are inundated. The Sió Valley: (c) large-scale meander, (d) anabranching channel, (e) small-scale meander.

(Hungary; Figures 5b and 5d). The river, canalized at the beginning of the nineteenth century, flows from Balaton Lake to the Danube River. The valley is surrounded by hills built of loess. Its catchment area measures ~9,200 km². The valley width varies from 1.5 to 3.0 km. The mean annual discharge in the Sió canal amounts to 39 m³ s⁻¹. The valley floor is filled with silts and sandy silts, delivered from loess hills surrounding the valley.

4.1. Data From Previous Studies in the Middle Obra and Sió Rivers

The grain-size data were used by Słowik (2014, 2016b) and Słowik et al. (2021) to determine trends in vertical changes of mean diameter and standard deviation of the Obra and Sió deposits. The grain-size distributions originated from analyses conducted using laser diffraction technique in a Malvern Mastersizer 3000 Hydro LV

(Malvern Inc., Malvern, United Kingdom) particle size analyzer (PSA) at the Szentágothai Research Centre, University of Pécs. In the present study, the grain-size distributions were used to determine the median grain-size D_{50} (Table 1) to plot this parameter with the values of stream power. The median grain-size was calculated using GRADISTAT 4.0 software (Blott & Pye, 2001). The valley slopes were estimated based on topographical maps and using "show elevation profile" and "distance measurement" tools available in Google Earth. The slopes were measured in valley sections with traces of the former channels.

Age estimation of paleochannel sediments in the middle Obra and Sió Valleys were published by Słowik (2014 – the Obra Valley), Słowik, Gałka and Marciniak (2020 – the Obra Valley), and Słowik et al. (2021 – the Sió Valley). Accelerator mass spectrometry (AMS) radiocarbon dating ($n = 32$) was carried out by Poznań Radiocarbon Laboratory ($n = 29$) and Gliwice Radiocarbon Laboratory ($n = 3$). Optically stimulated luminescence (OSL; $n = 18$) age determinations were done by the OSL laboratory in the Department of Physical Geography and Geoinformatics of the University of Szeged (Table 2). They allowed for determining the age of channel planforms identified in both areas. The age of the former channel, and the depths of dated sediments, were used to estimate aggradation rates for the middle Obra and Sió Valleys (Table 2).

Sediment dating provided the time scale of the preservation of the fluvial sedimentary record. All the samples used for AMS radiocarbon analyses were collected from apexes of paleomeanders. These channel sections provided relatively stable depositional conditions compared to limbs of paleomeanders filled by plug bars often reworked in periods of high flows (cf. Toonen et al., 2012). A stable deposition in meander apexes usually commences in an oxbow lake (marked by deposition of gyttjas) and is often followed by peatland formation (marked by deposition of peats). Information preserved within such sediments allows for detailed reconstructions of paleoenvironmental changes (e.g., Kołaczek et al., 2018). Moreover, our interpretations are based on extensive sets of radiocarbon data collected in the middle Obra and Sió Valleys, complemented in the Sió Valley by OSL dating.

The values of bankfull paleodischarges (Tables S3 and S4) were published in studies of Słowik (2018), Słowik, Gałka and Marciniak (2020), and Słowik et al. (2021) to determine the changes in the magnitude of flows in the identified channel planforms. In the present study, they were used to determine the values of stream power for particular generations of paleochannels identified in the Obra and Sió Valleys. The paleodischarges were estimated using the velocity-area method and Manning's formula (Morisawa, 1985) to determine the flow conveyed by the identified generations of paleochannels (Tables S3 and S4):

$$Q_b = v\,A_b \tag{3}$$

$$v = R^{2/3}\,S^{1/2}\,n^{-1} \tag{4}$$

where: Q_b – bankfull discharge ($m^3 s^{-1}$), v – mean velocity ($m\,s^{-1}$), A_b – cross-sectional area (m^2), R – hydraulic radius (m), S – channel slope, n – Manning's hydraulic roughness coefficient.

The values of the hydraulic radii were calculated using the formula:

$$R = A_b/P \tag{5}$$

where P is the wetted perimeter.

GPR images offer the possibility to image outlines of former channels in the Obra and Sió Valleys. The cross-sectional areas and wetted perimeters were calculated using GPR images shown in Słowik (2014), and Słowik, Gałka and Marciniak (2020). The imaging of the channels' shapes was possible owing to the difference in dielectric properties of peats and gyttjas filling the paleochannels, and mineral sediments forming their bottoms. In channels filled with mineral sediments the outline of the channel is often marked by a distinct reflection, produced by the difference between the grain-size of channel fill and bed sediments. When the reflections marking the bottom parts of channels were weak, data from boreholes and coring helped identify the interface between channel fill and river bed deposits. Wetted perimeters were measured manually on the GPR images using the identified channel outlines. Next, a mesh of rectangles was placed on the GPR images to determine the cross-sectional areas. Each rectangle corresponded to 2.0 m^2. Paleochannels >100 m wide were covered with 5.0 m^2 rectangles. In the near-bed zone, where the rectangles were incomplete, surfaces of triangles and trapezoids were calculated to obtain a complete surface of a cross-section (see example in Figure S1). In cases when a former channel was

Table 2
AMS Radiocarbon and OSL Dates From the Middle Obra Valley (Poland) (Słowik, 2014; Słowik, Gałka & Marciniak, 2020) and Sió Valley (Hungary) (Słowik et al., 2021), and Estimated Aggradation Rates

Sample name/depth (cm)	Sediment	Material	Nr. Lab.	C14 date	Age (cal yr BP, 95.4%)	Aggradation rate (mm y^{-1})
Middle Obra valley – radiocarbon dates						
WachI 279–281	Coarse gyttja	Pinus sylvestris bud scales 2× + periderm, Betula sect. albae fruit ×1, charcoal pieces, wood, undefined bud scales ×2, Alnus glutinosa fruits ×2	Poz-98095	4,875 ± 35 BP	5,697–5,487	0.49
Wach III 178–179	Gyttja	Charcoal	Poz-98139	2,195 ± 30 BP	2,312–2,132	0.77
KAR2 209–210	Silt	Pinus sylvestris needle ×1, Betula sect. albae fruits ×2, Carex lasiocarpa fruits ×2, Carex sp. fruit ×1	Poz-98217	10,770 ± 50 BP	12,751–12,631	0.16
KAR2 324–327	Coarse gyttja	Pinus sylvestris periderm ×1, Betula sect. albae fruits ×9, Carex sp. fruit ×1, Apiaceae fruit ×1	Poz-98218	11,380 ± 60 BP	13,339–13,086	0.24
KARM 223–228	Sand with gyttja	Pinus sylvestris bud scale + Populus sp. bud scales ×6	Poz-104768	9,920 ± 50 BP	11,603–11,225	0.20
KAR7 323–325	Gytjja	Betula sect. albae fruits ×4 + fruit scales ×8, Betula pubescens fruit scales ×2	Poz-104770	11,140 ± 60BP	13,109–12,824	0.21
KAR19 192–196	Gytjja with sand	Betula sect. albae fruits ×10 + fruit scales ×4, Betula pubescens fruit scale ×1	Poz-104771	10,670 ± 50 BP	12,713–12,560	0.15
OST2 198–202	Gyttja	Betula pubescens 8 fruits + 10 fruit scales	Poz-104764	9,800 ± 50 BP	11,309–11,149	0.17
OST1 205–209	Silt with gyttja	Betula sect. albae 6 fruits +12 fruit scales	Poz-104765	11,590 ± 50 BP	13,548–13,300	0.15
OST3 91–97	Sand with gytjja	Charcoal and wood pieces, Mentha sp. seed, Ranunculus lingua fruit ×2, Betula sect. albae fruit ×1	Poz-104767	3,335 ± 35 BP	3,683–3,475	0.26
OST4 351–353	Calcareous gyttja with sand	Charcoal + Pinus sylvestris needle (fragm.)	Poz-104496	10,930 ± 50 BP	12,933–12,703	0.27
OST4 212–216	Gytjja	Schoenoplactus lacustris fruits ×4, Betula pubescens fruits scale, Betula sect. albae fruits ×6	Poz-104843	8,920 ± 40 BP	10,192–9,913	0.21
OST4 110–112	Gytjja	Alnus glutinosa fruits ×4, Betula sect. albae fruit ×1, charcoal pieces, Carex sp. - fruit	Poz-104845	1,475 ± 30 BP	1,408–1,306	0.80
BEL1 112–114	Gytjja with silt and sand	Trapa natans nut remains* *-possible reservoir effect	Poz-104842	5,780 ± 40 BP	6,671–6,483	0.17
BEL1A 198–200	Silt	Pinus sylvestris bud scale + periderm	Poz-104773	5,870 ± 50 BP	6,788–6,566	0.29
BEL2 96–98	Sand with gytjja	Alnus glutinosa cone	Poz-104841	3,315 ± 30 BP	3,614–3,495	0.27
BEL3 95–100	Peat	Pinus sylvestris needle, Carex rostrata fruits ×3, Betula sect. albae fruit ×2	Poz-104769	9,360 ± 50 BP	10,713–10,427	0.14
BEL4 157–161	Gytjja with sand	Cirsium sp. fruit ×1 + charcoal pieces	Poz-104413	5,950 ± 40 BP	6,883–6,676	0.30
BEL4A 102–104	Gytjja with silt	Charcoal pieces	Poz-104772	5,940 ± 40 BP	5,940–6,671	0.17
Kopanica-11 140–145	Peat	N/A	GdS-1462	9,190 ± 120 BP	10,709–10,159	0.13
Kopanica-12 175–180	Peat	N/A	GdS-1465	4,730 ± 100 BP	5,661–5,071	0.24
Kopanica-13 75–80	Peat	N/A	GdS-1480	6,690 ± 100 BP	7,736–7,421	0.10
Sió valley – radiocarbon dates						
MED 8 294–302	Gyttja	Betula sect. albae fruits and fruits scales, wood piece, Pinus sylvestris periderm	Poz-111365	10,950 ± 60 BP	12,981–12,712	0.25

Table 2
Continued

Sample name/depth (cm)	Sediment	Material	Nr. Lab.	C14 date	Age (cal yr BP, 95.4%)	Aggradation rate (mm y^{-1})
MED 8 273–277	Gyttja	Betula sect. albae fruits and fruits scales, charcoal pieces, Pinus sylvestris needles	Poz-111366	9,810 ± 50 BP	11,317–11,166	0.24
MED 8 193–197	Gyttja	charcoal pieces, bud scales	Poz-111224	7,890 ± 40 BP	8,975–8,590	0.24
MED 8 153–161	Gyttja	Ranunculus sceleratus fruits, Urtica dioica fruits<i,></i> charcoal pieces	Poz-111368	6,510 ± 40 BP	7,495–7,323	0.21
MED 33 68–73	Silt	Scheonoplectus lacustris fruits	Poz-111369	1,025 ± 30 BP	1,025–804	0.71
MED 33/1 60–65	Silt	Oeanthe aquatica fruits	Poz-111370	1,125 ± 30 BP	1,173–959	0.55
MED 35 314–320	Gyttja	Lycopus europaeus fruits, Taraxacum sp. seed, bud scales	Poz-111372	8,740 ± 50 BP	9,903–9,555	0.32
MED 35 260–266	Gyttja	charcoal pieces, bud scales, Ranunculus sceleratus fruits	Poz-111373	8,120 ± 50 BP	9,262–9,891	0.26
MED 54 105–111	Gyttja	Scheonoplectus lacustris fruits, Ranuculus sp. fruit	Poz-111374	1,045 ± 30 BP	1,050–921	1.00
MED 54/1 72–76	Peat	Scheonoplectus lacustris fruits, Ranuculus sp. fruit, Alisma sp. - fruit	Poz-111375	995 ± 30 BP	964–798	0.78

Sió valley – OSL dates

Sample name/depth (cm)	Nr. Lab.	Water content (%)	Age model	U (ppm)	Th (ppm)	K (%)	D* (Gy/ka)	De (Gy)	Age	Aggradation rate (mmy^{-1})
MED23/80	OSZ 1753	19	MAM	1.85 ± 0.02	5.34 ± 0.09	0.92 ± 0.04	1.6 ± 0.11	3.1 ± 0.23	1,940 ± 20	0.41
MED25/70	OSZ 1754	22	CAM	2.23 ± 0.03	6.47 ± 0.12	1 ± 0.04	1.84 ± 0.12	0.64 ± 0.04	350 ± 30	2.00
MED25 PB/60	OSZ 1755	17	CAM	2.55 ± 0.03	7.67 ± 0.14	1.06 ± 0.04	2.03 ± 0.12	0.61 ± 0.02	300 ± 20	2.00
MED25 PB/140	OSZ 1756	18	CAM	1.76 ± 0.02	5.08 ± 0.09	0.09 ± 0.03	1.57 ± 0.12	0.54 ± 0.035	340 ± 30	4.11
MED46 B/90	OSZ 1757	17	CAM	1.92 ± 0.02	5.48 ± 0.1	0.93 ± 0.04	1.65 ± 0.12	1.02 ± 0.05	620 ± 50	1.45
MED46 B/110	OSZ 1758	18	CAM	1.92 ± 0.02	5.48 ± 0.1	0.93 ± 0.04	1.64 ± 0.12	1.17 ± 0.06	710 ± 60	1.54
MED46 T1/110	OSZ 1759	23	CAM	2.81 ± 0.03	8.18 ± 0.15	1.16 ± 0.04	2.07 ± 0.11	2.07 ± 0.08	1,000 ± 70	1.10
MED46 T2/100	OSZ 1760	10	MAM	1.87 ± 0.04	5.58 ± 0.15	0.92 ± 0.03	1.74 ± 0.14	21.96 ± 1.33	12,610 ± 930	0.07
MED9 CH/70	OSZ 1761	18	CAM	2.44 ± 0.03	7.26 ± 0.13	0.86 ± 0.03	1.79 ± 0.12	1.92 ± 0.09	1,080 ± 90	0.64
MED9 PB/200	OSZ 1763	15	CAM	1.24 ± 0.02	3.55 ± 0.07	0.82 ± 0.03	1.31 ± 0.12	20.64 ± 0.52	15,730 ± 1,550	0.71
MED13 CH/50	OSZ 1764	16	CAM	1.02 ± 0.01	3.08 ± 0.07	0.82 ± 0.03	1.26 ± 0.12	1.23 ± 0.03	980 ± 90	0.51
MED30 CH/100	OSZ 1765	17	MAM	1.94 ± 0.02	5.75 ± 0.1	0.98 ± 0.04	1.71 ± 0.12	9.98 ± 0.49	5,830 ± 50	0.17
MED30 PB/110	OSZ 1766	7	CAM	1.8 ± 0.02	5.3 ± 0.1	0.87 ± 0.03	1.87 ± 0.08	21.83 ± 0.57	11,650 ± 580	0.09
MED30 PB/210	OSZ 1767	16	CAM	2.9 ± 0.03	8.58 ± 0.15	0.94 ± 0.04	2.04 ± 0.12	25.73 ± 0.84	12,640 ± 880	0.16
MED46 T1/170	OSZ 1768	19	CAM	1.97 ± 0.02	5.69 ± 0.1	0.98 ± 0.04	1.67 ± 0.12	2.85 ± 0.05	1,700 ± 120	0.10
SZ1/60	OSZ 1814	20	CAM	0.73 ± 0.01	2.25 ± 0.05	0.85 ± 0.03	1.13 ± 0.11	1.65 ± 0.07	1,380 ± 140	0.43
SZ1/110	OSZ 1815	10	CAM	0.73 ± 0.01	2.25 ± 0.05	0.85 ± 0.03	1.22 ± 0.07	1.81 ± 1.59	1,480 ± 130	0.74
SZ2/190	OSZ 1817	20	CAM	2.22 ± 0.03	6.45 ± 0.12	0.95 ± 0.04	1.72 ± 0.11	31.03 ± 0.96	18,050 ± 1,330	0.10

situated lower than the adjacent point bar, its cross-sectional area was determined in reference to the upper part of the point bar to estimate the values corresponding to bankfull conditions.

4.1.1. Estimations of Manning's *n* Coefficient

Manning's *n* coefficients were estimated for the middle Obra Valley by Słowik, Gałka and Marciniak (2020), and for the Sió Valley by Słowik et al. (2021), based on tables provided by Acrement and Schneider (1989). The aim was to estimate bankfull paleodischarge conveyed by the types of channel planforms identified in both valleys.

Hydraulic roughness coefficient describes the frictional resistance exerted by the bed and banks of natural rivers on flow. Elements influencing its values were characterized by Chow (1959 in: Roggenkamp & Herget, 2000):

$$n = (n_1 + n_2 + n_3 + n_4 + n_5 + n_6 + n_7 + n_8 + n_9)\, m \tag{6}$$

where n_1 refers to surface roughness caused by the grain-size of sediments at the bottom of the river bed, n_2 represents the influence of vegetation on flow conditions, n_3 describes channel irregularity caused by bedforms, n_4 refers to channel alignment (generated by differences of the river banks from the straight line), n_5 is the effect of obstructions (logs, stumps, dams, bridges, etc.). Elements n_6–n_9 characterize silting and scouring, stage and discharge, sediment load, and seasonal changes, respectively. Element "m" is a correction factor for channel meandering.

Owing to the intervals in particular n-elements (see Acrement & Schneider, 1989), three discharge values (minimum, average, and maximum discharge) were estimated for particular types of former channels, identified in the middle Obra and Sió Valleys (Tables S3 and S4). The average paleodischarge values were then used to calculate potential specific stream power in the middle Obra and Sió Rivers.

Element n_1 was determined based on the grain-size of sediment samples collected from the bottom of paleochannels. The effect of vegetation (n_2) was estimated as "small" for paleochannels active in the Late Glacial in both valleys, and "medium" for anabranching and meandering channels active in the Holocene. Channel irregularity caused by bedforms (n_3) was determined as "minor" for meandering and sinuous channels owing to small or no traces of bedforms and eroding and reworking of the channels identified in the GPR images. The exception was anabranching and crevasse channels owing to the presence of bed forms and erosional surfaces. Channel alignment (n_4) was negligible or small as variations in channels widths were gradual or large and small cross-section alternated occasionally. This element was inferred from aerial images (source: Google Earth), in which traces of former channel planforms could be identified. The effect of obstructions (n_5) was defined as negligible, for example, in meanders from the Late Glacial. It was classified as appreciable the case of anabranching channels in the middle Obra Valley because traces of buried objects (possibly logs) were identified in the GPR images. In the case of crevasse channels, the effect was "severe" as traces of a dam impeding the flow were spotted on the land surface. Element 'm' was defined based on the values of sinuosity.

The roughness coefficients in the middle Obra and Sió Valleys are comparable for the large-scale meanders (see Table S3). In the case of anabranching channels – those evolving in the middle Obra Valley are characterized by higher values of Manning's n coefficient owing to a higher value of n_5 (effect of obstructions – more buried objects in the channel fills, possibly tree logs) compared to the Sió Valley (Table S3). Small–scale meanders have higher roughness in the Sió Valley compared to the middle Obra owing to a higher channel irregularity (numerous erosional surfaces appearing in the channel fills (cf. Słowik et al., 2021).

4.1.2. Standard Errors of Estimations

The estimations of potential specific stream power bear uncertainties delivered by errors in calculations of paleodischarges, Manning's roughness coefficients, and mean velocities (see Equations 1–4). To estimate these uncertainties for the middle Obra and Sió Valleys, we have calculated standard errors for these variables (see Table S4). They were estimated using the formula:

$$SE = SD / \sqrt{n} \tag{7}$$

where, SE – standard error, SD – standard deviation, and n – number of samples. Standard deviation was determined using the formula:

$$SD = \sqrt{\Sigma(\chi_i - \mu)^2 / n - 1} \tag{8}$$

where, χ_i is each value for population, and μ is the mean for the population. The samples used for the estimations of standard error and standard deviation originate from multiple locations representing similar types of former channel planforms, active in a similar period (Table S4).

The highest errors refer to the highest volumes of paleodischarge conveyed by large-scale meanders in the middle Obra and Sió Valleys. They reach 25 for the average discharge of 108 m³ s⁻¹ (the middle Obra River), and 88 for 335 m³ s⁻¹ (the Sió River). This means that the estimated values of the paleodischarge vary between 247 and
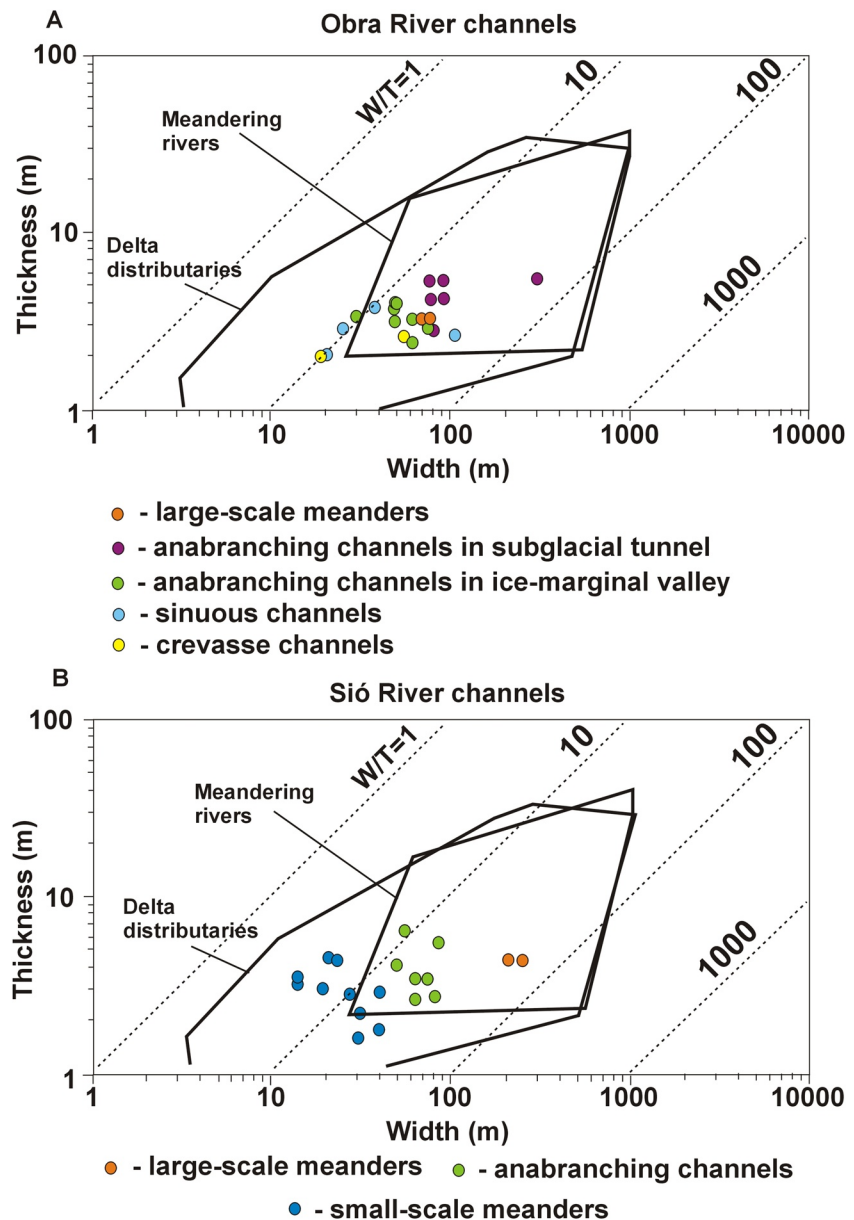
Figure 8. Width, thickness and types of channel planforms identified in the middle Obra (a) and Sió Valley (b) plotted on diagrams proposed by Gibling (2006). The widths and thickness of the channels were measured in the GPR images carried out by Słowik (2013, 2014), Słowik, Gałka and Marciniak (2020), and Słowik et al. (2021). Aerial images (source: Google Earth) were an additional source to determine the channel widths.

423 $m^3 s^{-1}$ (335 $m^3 s^{-1}$ ± 88). The error covers 52% of the average value of the paleodischarge. For relatively small discharge values conveyed by small-scale meanders (e.g., 13 $m^3 s^{-1}$) the standard error amounts to 2. Here the error (13 $m^3 s^{-1}$ ± 2) amounts to 39% of the estimated discharge value. In general, the higher the values and range of the variables, the higher the value of the standard errors. This shows that the estimated stream power can be treated as approximate owing to the high standard errors. Therefore, the observed trends in stream power changes were supported with plots of the age of former channels and valley width/channel belt width ratios.

4.2. Width and Thickness of Channel Fills

The width and thickness of large-scale meanders preserved in the middle Obra Valley are 70–80 and 4 m, respectively (Figure 8a, Table 1). The anabranching channels formed within a former subglacial tunnel, have widths
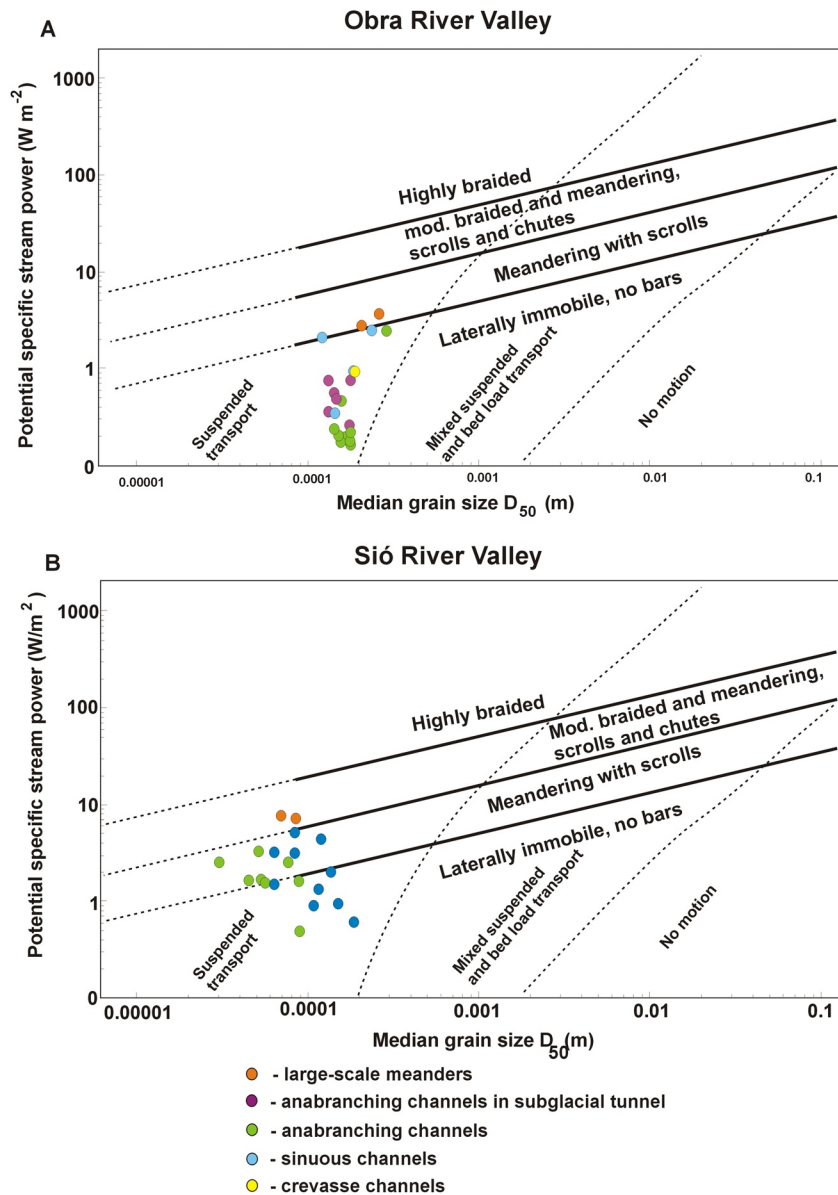
Figure 9. Potential specific stream power and median grain-size of paleochannels preserved in the middle Obra (a) and Sió Valley (b) plotted in a diagram discriminating channel planforms and types of sediment transport proposed by Kleinhans and van den Berg (2011). The values of stream power were estimated using bankfull paleodischarge estimated by Słowik, Gałka and Marciniak (2020), and Słowik et al. (2021) (see Table 1). The valley slope was measured on topographic maps. The median grain-size was calculated using GRADISTAT 4.0 software (Blott & Pye, 2001). The input data were grain-size distributions obtained from analyses conducted at the Szentágothai Research Centre, University of Pécs.

and depths of 120 and 5 m, respectively. The anabranching and sinuous channels, formed after the transition from large-scale bends in the middle Obra Valley, are 50–70 m wide and 2.5–3.0 m thick (Figure 8a). The width of the channel fills in the Sió valley decrease from large-scale meanders (100–120 m), through anabranching channels (60–90 m) to small-scale bends (15–40 m; Figure 8b). A decrease in the channel thickness can also be noted (Figure 8b).

4.3. Stream Power of Channel Planforms Preserved in the Fluvial Record

Large-scale meanders and part of sinuous channels in the middle Obra Valley were characterized by specific stream power of 2.0–3.0 W m^{-2} (Figure 9a). When plotted with median grain-size, the channels belonged to

meandering rivers with scrolls and chutes (Figure 9a). All the anabranching channels were classified as "laterally immobile, no bars." Specific stream power of 7.0–8.0 W m^{-2} describes large-scale meanders in the Sió Valley (Figure 9b). The stream power of anabranching channels and small-scale meanders amounts to 1.0–3.0 W m^{-2}. The multi-channel planform, and part of the small-scale bends belong to the zone "meandering with scrolls and chutes" (Figure 9b; cf. Kleinhans & van den Berg, 2011). Both middle Obra and Sió Rivers are dominated by a suspended load (Figure 9). The grain size of the Sió sediments is an order of magnitude finer (between 0.00001 and 0.0001 m – from silts to very fine sands) than sediments forming the Obra alluvial fill (0.0001–0.001 m – from very fine sands to coarse sands; see Figure 9). The exception is small-scale bends in the Sió Valley that, owing to bed incision reworked coarser deposits present in the valley floor (cf. Słowik et al., 2021).

4.4. Changes in Stream Power, Channel Belt Width, and Planform Evolution of the Middle Obra and Sió Rivers

A decrease of stream power from 2.0 to 3.0 W m^{-2} to 0.1–0.8 W m^{-2} accompanied the transition from large-scale meanders to anabranching and sinuous channels in the middle Obra Valley between 13,300 and 11,200 cal. yr BP (Słowik, Gałka & Marciniak 2020). Valley width/channel belt width ratio increased from 7.0 to 9.0 to 25.0 in that period (Figure 10c). The anabranching channels were active between ∼11,000 cal. yr BP and the nineteenth century. Aggradation rates amounted to 0.1–0.2 mm y^{-1} (with a maximum of 0.8 mm y^{-1}) between 11,000 and 4,000 cal. yr BP (Figure 10c). In this period, the valley width/channel belt width ratio ranged from 22.5 to 25.0 (see Table 1). A temporary increase in stream power to 2.0 W m^{-2} occurred ∼3,800 cal. yr BP. Aggradation rates increased to 0.3–0.8 mm y^{-1}. Valley width/channel belt width ratio remained constant at that time (∼22.0; Figure 10c).

The transition from large-scale meanders to anabranching planform in the Sió Valley ∼18,000 cal. yr BP was accompanied by the decrease in specific stream power from 7 to 8 W m^{-2} to 1.0–3.0 W m^{-2} (Figures 10b and 10c). Valley width/channel belt width ratio amounted to 1.0 when the large-scale bends were active and increased to 1.5–1.8 after the transition to the multi-channel planform. Aggradation rates increased from 0.1 mm y^{-1} to 0.1–0.3 (maximum 0.7) mm y^{-1} (Figure 10c). The change of channel planform from the anabranching channels to small-scale meanders took place ∼12,700 cal. yr BP and was accompanied by sustaining potential specific stream power of 1.0–3.0 W m^{-2} (Figure 10c). The stream power was sustained; however, the transition was accompanied by the reduction of bankfull flows to 6.0–12.0 m^3 s^{-1} (Table S4 and Słowik et al., 2021), a decrease in channel width (Figure 8b), and an increase in valley width/channel belt width ratio to 7.9–8.1 (Figure 10b). The small-scale meanders incised. Aggradation rates amounted to 0.1–0.3 mm y^{-1} between 12,000 and 6,000 cal. yr BP (Figure 10c), and increased to 1.0–4.0 mm y^{-1} during the last ∼2,000 cal. yr BP.

5. Discussion

5.1. Conditions to Preserve Channel Planform Record in the Obra and Sió Valleys

The sedimentary record of channel planforms preserved in the middle Obra and Sió Rivers confirms the hypothesis that a decrease in potential specific stream power followed by sustained low stream power, and successive decrease of channel belt width results in maintaining the sedimentary record of channel planforms over 10^3 to 10^4-year time scales. In the Sió Valley, the planform change is accompanied by the decrease in stream power, increased aggradation (Figure 10c), successive decrease of the width and depth of the channels (Figure 9b), and decrease in width of channel belts (Figure 10c). These trends are not so clear in the middle Obra Valley (Figure 8a). This is because large-scale meanders did not rework the whole Obra valley floor. The river flows through the Warsaw-Berlin proglacial stream valley, formed by the activity of glacial meltwater flows. Part of the channels (i.e., anabranching channels in the bifurcation to the Warta River; Słowik, Gałka, & Marciniak, 2020) evolved within larger channel forms inherited from glacial meltwater flows across outwash plains and former subglacial tunnels. A decrease of flows and stream power caused sedimentary structures, that is, fragments of point bars, sets of small bedforms, and smaller-scale channels have been preserved within the 120-m wide channels formed by the meltwater flows (see Figure 4 and II in Słowik, Gałka & Marciniak, 2020). Compared to the Sió Valley, the relatively high values of valley width/channel belt width ratio for the Obra large-scale meanders (∼7.0–9.0) show that a significant part of the valley fill contains the fluvioglacial record left by meltwater of the last Inland Ice or is occupied by glacial and aeolian landforms (see Figure 5).
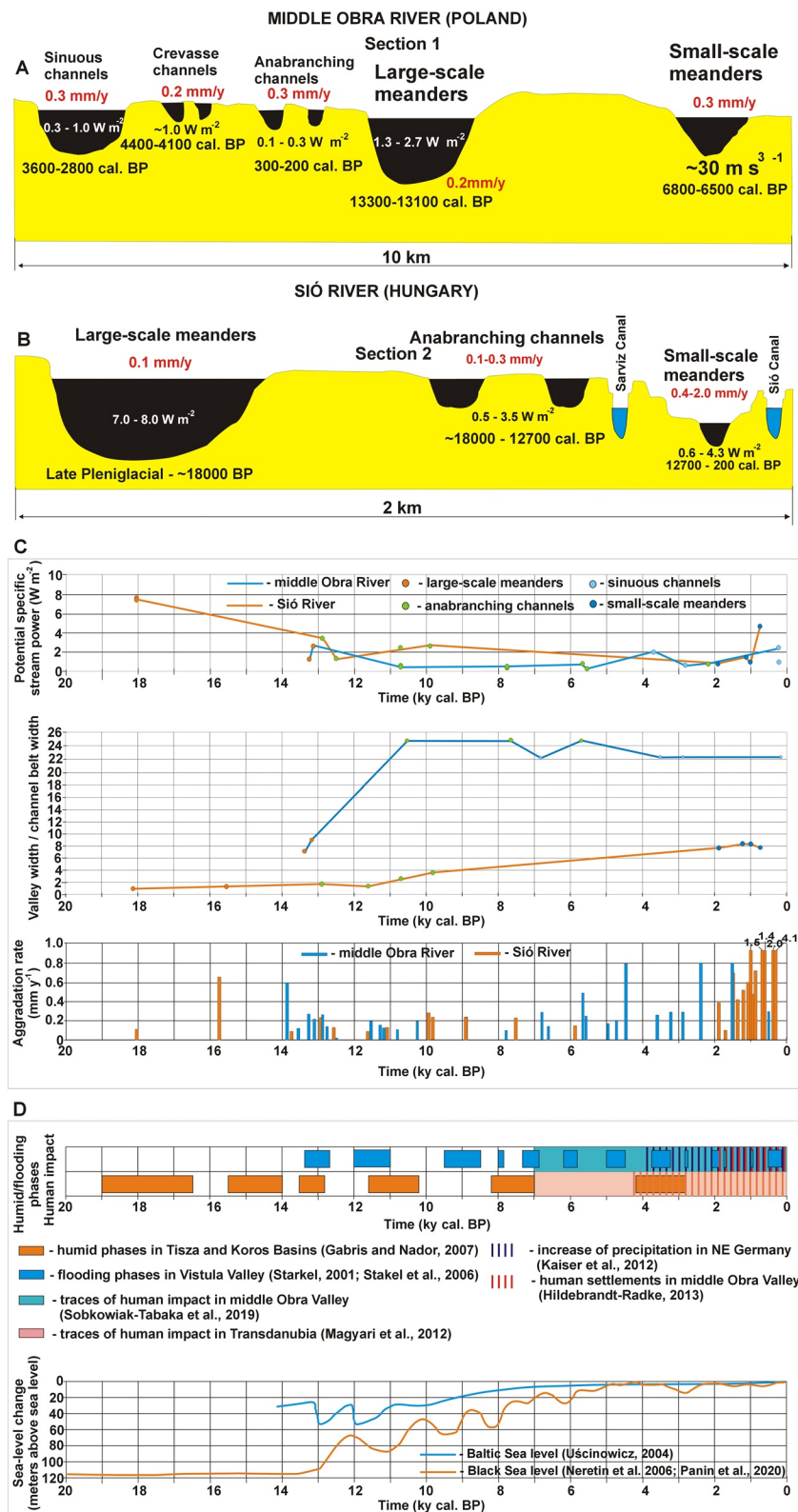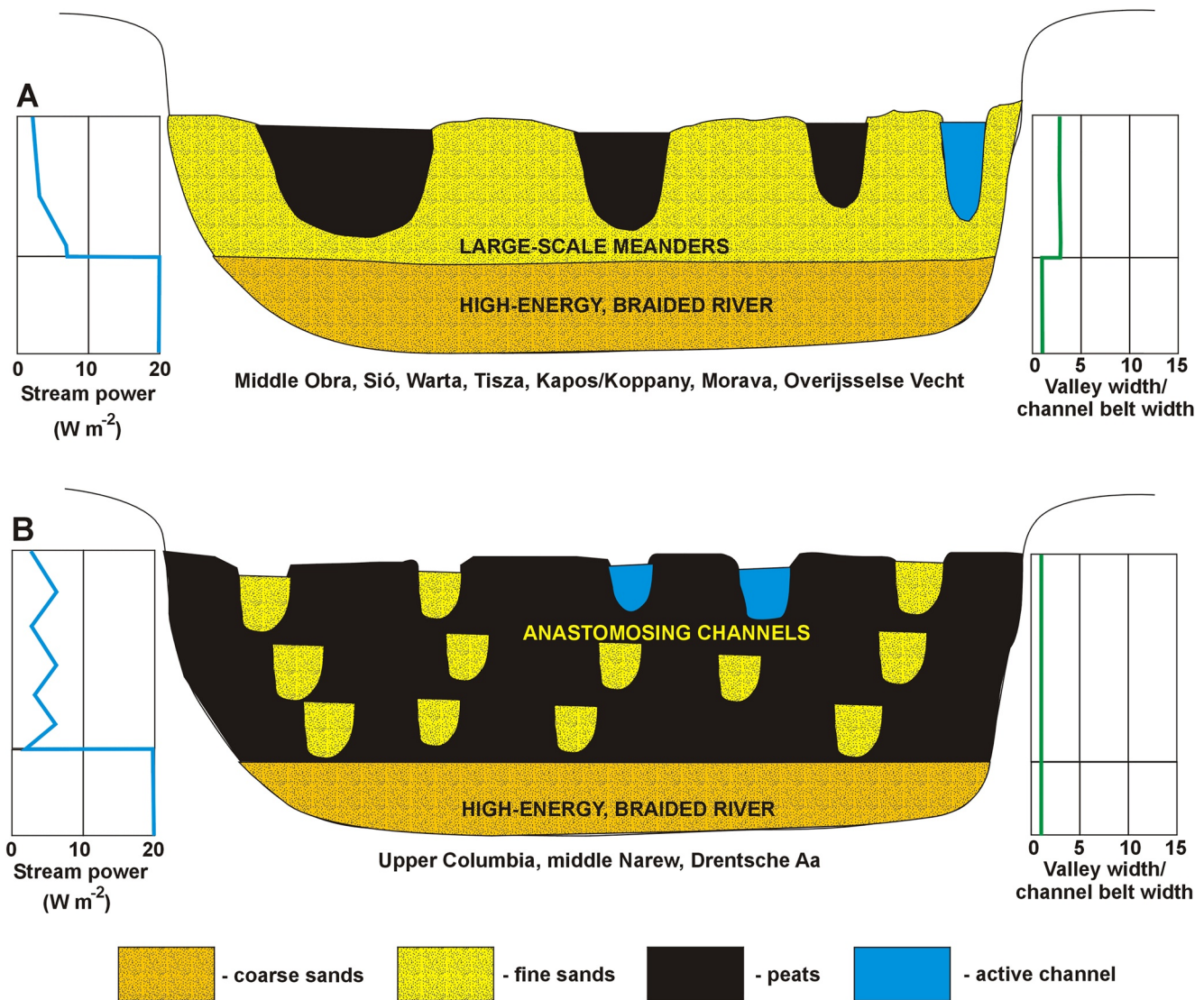
Figure 10.

Figure 11. Vertical changes in stream power and channel belt width in fluvial record (a) coarse sediments of high-energy braided river overlain by the record of meandering planforms, (b) coarse sediments of high-energy braided river overlain by the record of meandering planforms.

The change from large-scale meanders to anabranching and sinuous planforms in Obra Valley is reflected by the change in fluvial architecture - from multi-storey, represented by fills of the large-scale meanders, to erosion and succession dominated in the cases of the anabranching channels (cf. Gibling, 2006; see e.g., Figures 4 and 5 in Słowik, 2013, and Figures 4 and 5 in Słowik, Gałka & Marciniak, 2020). The planform transition was caused by the lowering of the base level, and a period of increased floods (Figure 10d). The anabranching and sinuous channels in the middle Obra Valley, and anabranching channels and small-scale meanders in the Sió Valley, are situated close to the border between meandering rivers and delta distributaries marked by Gibling (2006) (see Figure 8). This is consistent with the important role of avulsions, bifurcations and meander cutoffs in the evolution of both rivers.

Figure 10. (a, b) Schematic cross-sections showing types of channel planforms in the middle Obra and Sió Valleys. They were constructed based on the GPR measurements ground-truthed by sedimentary data from coring (Słowik, Gałka & Marciniak, 2020; Słowik et al., 2021), topographic maps and aerial images (aerial survey conducted on 1 April 2010, and Google Earth images). (c) Potential specific stream power, valley width/channel belt width ratio, and aggradation rate plotted with the age of paleochannels in the middle Obra and Sió Valleys. (d) Base-level changes, the occurrence of flooding/humid phases, and human impact in the middle Obra and Sió Valleys during the last 20,000 cal. BP.

The increase in stream power and sedimentation rates ~3,800 cal. yr BP was influenced by periods of flooding (Starkel, 2001; Starkel et al., 2006; see Figures 10c and 10d). The occurrence of the flooding phases was affected by the increase of precipitation and humidity in the European lowlands (e.g., Kaiser et al., 2012, and references therein; Lamentowicz et al., 2015). Moreover, traces of the presence of humans ~7,000 cal. yr BP were found in the western part of the middle Obra Valley by Sobkowiak-Tabaka et al. (2019). They were marked by types of pollen characteristic of open areas in the forest, species of algae indicative of trophic conditions in lakes, erosional processes in lake catchments, and charred fragments of herbaceous plants derived from marsh vegetation. First human settlements, and potential deforestation accompanied by soil erosion, appeared in the central and eastern part of the middle Obra Valley ~2,000 cal. yr BP (Hildebrandt-Radke, 2013). These events could have contributed to increased runoff and sedimentation in valley floors. Along with the human-induced changes, this sedimentation was also influenced by the increase of the base level, conditioned by the rise of the Baltic Sea level (Uścinowicz, 2004; Figure 10d).

In the Sió Valley, the change from the large-scale meanders to anabranching channels took place during a humid phase that took place between 13,500 and 12,700 cal. yr BP, identified by Gábris and Nádor (2007) (Figure 10d). The reduction of the stream power was affected by a decrease in bankfull discharge from ~250 m^3 s^{-1}, conveyed by the large-scale meanders, to ~10–30 m^3 s^{-1}, conveyed by the anabranching channels (Table S4). These changes could have been affected by the rise of the local base level, caused by an intensive sedimentation in the Pannonian Basin (Kasse et al., 2010; Nowaczinski et al., 2015; see Figure 5 for location). This sedimentation could have been interrupted by periods of incision of the Danube River (Pécsi, 1959). The situation of the anabranching channels from the Sió Valley in the "meandering with scrolls and chutes" zone of the diagram of Kleinhans and van den Berg (2011) (see Figure 9b) is in agreement with the study of Słowik et al. (2021) that the anabranching channels evolved through lateral migration, chute cutoffs, and formation of "soft avulsions" maintaining the flow in original channels after cutoff events. The situation of the anabranching channels in the middle Obra Valley ("laterally immobile, no bars"; Figure 9a) informs that they were less mobile than the multi-channel planform in the Sió Valley. Indeed, they have no or few traces of lateral migration compared to the Sió anabranching channels, featured with numerous traces of lateral migration, marked by layering patterns preserved in the floodplain (see Figure S2).

The small-scale meanders evolved through lateral migration and cutoffs (cf. Słowik et al., 2021). Their incision could have been caused by a temporary decrease of the local base-level, conditioned by the incision of the Danube River (Pécsi, 1959). This incision, in turn, could have been affected by a decrease of the Black Sea level between 12,000 and 11,000 cal. yr BP (Neretin et al., 2006; Panin et al., 2020 – see Figure 10d). The local base level further decreased ~5,000 cal. yr BP owing to the incision of the Danube River (Tóth et al., 2017). Despite this event, an increase of aggradation to 1.0–4.0 mm y^{-1} took place during the last ~2,000 cal. yr BP and was caused by the anthropogenic influence (deforestation, burning for pastures) that started in Transdanubia 7,000–6,500 cal. BP (Magyari et al., 2012; Figure 10d). The human influence was coupled with a humid period that started in central and eastern Europe about 4,000 cal. yr BP (Gałka et al., 2018; see also a humid phase identified by Gábris & Nádor, 2007, marked in Figure 10d).

5.2. Applications of the Results

Based on the present study, river valleys with the record of at least two generations of channel planforms, and valley width/channel belt width ratios between 6 and 12, are potential sites preserving fluvial sedimentary record over 10^3 to 10^4-year time scales. This is supported by the observed increase of valley width/channel belt width ratios after the transitions from large-scale meanders to low-energy meandering and anabranching rivers from 1 to 2 in the Late Glacial to 6–12 in the Holocene (Figure 2a2). The observed trends are the result of the successive decrease in stream power. The decrease was caused by the termination of delivery of glacial meltwater from the last Inland Ice, the appearance of a dense vegetation cover, and "using" part of the available water by evapotranspiration as climate warmed (cf. Rotnicki, 1991).

The proposed classification may be extended by avulsive river systems formed in coastal zones and affected by the backwater effect owing to sea-level rise (cf. Chatanantavet et al., 2012). They may belong to the second of the identified groups of rivers (see Section 3.2). The examples are the anastomosing course of the lower Odra River (Poland) formed ~7,000 cal. yr BP; Duda & Borówka, 2007), and lower Prieglius River (Lithuania). The proposed framework can also be extended by channel planform records preserved in the floodplains of large

rivers. For instance, the Mississippi Valley near New Madrid contains traces of numerous paleomeanders with traces of 16 periods of reworking earlier records and cutoffs (Durkin et al., 2018). The channels are fragmentary (valley width/channel belt width ratio can be close to 1.0 based on Figures 11a and 11b in Durkin et al., 2018), with the most complete preservation of meanders representing the stage that took place at 500 cal. yr BP. These features show that the section of the Mississippi Valley near New Madrid may belong to the group of actively migrating rivers (Section 3.3). Moreover, rivers classified to one of the identified groups may have sections that indicate a higher preservation potential than indicated by the main trajectory of channel planform changes. For instance, the whole valley width of the South Saskatchewan River (high-energy braided rivers – Section 3.4) is occupied by braided channels near the town of Outlook. The valley section situated close to Saskatoon preserves traces of paleomeanders along the valley margins (see Figure S3). The age of the paleomeanders and the nature of changes in the preservation potential along this river course require a detailed field study.

The proposed framework of rivers has the potential to be extended by ancient fluvial records. For instance, the Early Cretaceous record of river meanders found in the McMurray Formation (Alberta, Canada; Durkin et al., 2018) may belong to the group of actively migrating rivers (Section 3.3) owing to traces of cutoffs, often reworking the earlier record, and preservation of a low-sinuosity channel section (see Figures 7a and 7b in Durkin et al., 2018). We conducted a Welch's t-test to verify whether the sinuosity of ancient channel records is distinguishable from channel belts preserved in the surface layers of the floodplains (see Tables S1 and S2). The test indicated that the difference between the sinuosity of the two groups of rivers is not statistically significant at the 95% confidence interval. This suggests that the sinuosity of ancient channel belts may not undergo significant changes in planform shape after deposition in the floodplain sediments, if the deposits have already succeeded in being preserved at time scales of thousands to tens of thousands of years. These notions require further verification by more examples from the ancient fluvial record.

The observed changes in stream power and valley width/channel belt width ratio also refer to relations between the fluvial record preserved in the top parts of floodplains, and the underlying fluvial archives. The 10^3 to 10^4-years record of channel planforms often overlies deposits representing the activity of high-energy braided rivers (e.g., the Kapos and Koppány River - Lóczy & Dezső, 2013, Figure 11a; the Narew River – Gradziński et al., 2003; the upper Columbia River – Makaske et al., 2002, Figure 11b). These examples represent a vertical sedimentary record of a decrease in stream power during a transition from the braided planform to the overlying record of meanders or anastomosing channels (Figures 11a and 11b). Valley width/channel belt width ratios increased in the vertical record from 1.0 (the whole valley width occupied by the braided system) to 3.0 (large-scale meanders) in course of, for example, the Warta River, and 7.0–8.0 in the course of the middle Obra River. In all these cases the condition to preserve the underlying sedimentary record was that the successive river system (i.e., large-scale meanders or anastomosing system) was featured with lower flow energy than the underlying fluvial record (Figures 11a and 11b).

The findings of our study should be extended beyond the temperate zone. Little is known about controls on the preservation potential of dryland and tropical rivers, especially in intracratonic settings. For instance, the Cooper Creek Basin, Australia, contains traces of a suspended load-dominated anabranching planform that was active at 75,000–55,000 cal. yr BP (Jansen et al., 2013). The present anastomosing course (cf. Gibling et al., 1998) reworks only the surficial layer of the basin. Sediments filling the Amazon River basin were deposited by megafans and systems of avulsive channels coming from the Andes in the Late Miocene (9.0–6.5 Ma). They were reorganized into a transcontinental fluvial basin in the early Pliocene (cf. Latrubesse, 2015; Latrubesse et al., 2010). Detailed identification of the controls on the preservation over such long-time scales remains a challenge.

6. Conclusions

The main goal of our study was to identify a set of conditions that influence the preservation of channel planform records in the surface and subsurface of river floodplains prior to the maintenance of rock record. We tested a hypothesis that a successive decrease of stream power, accompanied by the increase of valley width/channel belt width ratio, favors the preservation of the sedimentary record of channel planforms over 10^3 to 10^4-year time scales. Our study is based on a literature review conducted in reference to temperate rivers of the Northern Hemisphere. We collected data regarding paleodischarge, width, and thickness of paleochannels, grain-size, valley

widths, channel belt widths, and age of paleochannels preserved in the valley floors. These data were used to estimate specific stream power for generations of paleochannels preserved in the river floodplains.

We developed a framework consisting of four groups of rivers with preservation potentials varying from thousands and tens of thousands years to annual time scales. We found that a decrease of stream power followed by a low stream power, accompanied by a decrease of channel belt widths in successive generations of channel planforms favored the preservation of channel planform records over 10^3 to 10^4 ky time scales. Our study shows that river valleys characterized by valley width/channel belt width ratios between 6 and 12, and traces of channels representing at least two generations of channel planforms, are potential areas containing the preservation of channel planform sedimentary record in thousands to tens of thousands year time scales. Low and moderate energy (0.5–45.0 W m^{-2}), meandering and anastomosing rivers with constant channel belt widths preserve the sedimentary record of channel planforms from the last 4,000–7,000 years. They are characterized by periods of increased stream power, contributing to the formation of avulsions. Aggrading conditions lead to the preservation of vertically stacked channel fills. Moderate and high energy (30–170 W m^{-2}) meandering and anabranching rivers and high-energy (60–700 W m^{-2}) braided rivers preserve traces of former channels in centennial and annual to decadal time scales, respectively.

We analyzed in detail the conditions that led to the preservation of 10^4-year fluvial records of channel planforms using examples of unusually well-preserved paleochannels from the middle Obra River (western Poland) and Sió River (southern Hungary). They represent a sedimentary record of channel planforms reaching back to the Late Glacial and Late Pleniglacial, respectively. Specific stream power decreased from 2.0 to 3.0 W m^{-2}–13,000 cal. yr BP to <1.0 W m^{-2} between 11,000 and 4,000 cal. yr BP in the Obra Valley. A decrease from 7.0 to 8.0 W m^{-2}–18,000 BP to 1.0–3.5 W m^{-2} between 13,000 and 1,000 cal. yr BP took place in the Sió Valley. The decrease was caused by the reduced magnitude of flows, development of vegetation cover, and increase in evapotranspiration in the early and middle Holocene. The maintained low stream power went along with the sustained level of aggradation rates, caused by sediment delivery from moraine uplands and loess hills, and successive increase of the base-level, conditioned by the Baltic and the Black Sea levels. The aggradation increased during the last 2,000–3,000 cal. yr BP both in the Obra and Sió Valley owing to increased human impact and climate humidity.

The proposed framework can be extended by examples of paleochannels preserved in floodplains of large rivers, and coastal river valleys. Channel planforms preserved in ancient rock records also may be included in the framework, providing further research on how their geometry is altered by post-depositional processes (i.e., compaction). Extending our results concerning rivers evolving in other geomorphic zones would allow for the identification of controls on preservation of fluvial records in multi-millennial time scales.

Data Availability Statement

All data sets from this research are available from the ZENODO repository, https://doi.org/10.5281/zenodo.6104451. Part of the data, regarding estimations of hydraulic roughness coefficients and paleodischarges, is available in Słowik (2013), Słowik et al. (2020) and Słowik et al. (2021).

Supporting Information

Tables S1–S4 can be found in supplementary material https://doi.org/10.5281/zenodo.6104451

References

Acrement, G. J., & Schneider, V. R. (1989). Guide for selecting Manning's roughness coefficients for natural channels and floodplains. *US Geological Survey Water-Supply Paper*, *2339*, 1–37.

Allen, J. R. L. (1984). *Sedimentary structures, their character, and physical basis*. Elsevier.

Ashworth, P. J., Sambrook Smith, G. H., Best, J. L., Bridge, J. S., Lane, S. N., Lunt, I. A., et al. (2011). Evolution and sedimentology of a channel fill in the sandy braided South Saskatchewan River and its comparison to the deposits of an adjacent compound bar. *Sedimentology*, *58*, 1860–1883.

Bábek, O., Sedáček, J., Novák, A., & Létal, A. (2018). Electrical resistivity imaging of anastomosing river subsurface stratigraphy and possible controls of fluvial style change in graben-like basin, Czech Republic. *Geomorphology*, *317*, 139–156.

Bagnold, R. A. (1966). *An approach to the sediment transport problem from general physics* (Vol. 422-I, p. 43). Geological Survey Professional Paper.

Bertoldi, W., Gurnell, A., Surian, N., & Tockner, K. (2009). Understanding reference processes: Linkages between river flows, sediment dynamics and vegetated landforms along the Tagliamento River, Italy. *River Research and Applications*, *25*, 501–516.

Bertoldi, W., Zanoni, L., & Tubino, M. (2010). Assessment of morphological changes induced by flow and flood pulses in a gravel bed braided river: The Tagliamento River (Italy). *Geomorphology*, *114*, 348–360.

Blom, A. (1997). *Planform changes and overbank flow in meandering rivers: the river Allier* (pp. 1–345) [Ph.D. dissertation]. Delft University of Technology.

Blott, S. J., & Pye, K. (2001). GRADISTAT: A grain size distribution and statistics package for the analysis of unconsolidated sediments. *Earth Surface Processes and Landforms*, *26*, 1237–1248.

Blum, M. D., & Törnqvist, T. E. (2000). Fluvial responses to climate and sea-level change: A review and look forward. *Sedimentology*, *47*, 2–48.

Bridge, J., & Best, J. (1997). Preservation of planar laminae due to migration of low-relief bed waves over aggrading upper-stage plane beds: Comparison of experimental data with theory. *Sedimentology*, *44*, 253–262.

Candel, H. J. H., Kleinhans, M. G., Makaske, B., Hoek, W. Z., Quik, C., & Wallinga, J. (2018). Late Holocene channel pattern change from laterally stable to meandering – A palaeohydrological reconstruction. *Earth Surface Dynamics*, *6*, 723–741.

Candel, J. H. J., Makaske, B., Storms, J. E. A., & Wallinga, J. (2017). Oblique aggradation: A novel explanation for sinuosity of low-energy streams in peat-filled valley systems. *Earth Surface Processes and Landforms*, *42*, 2679–2696.

Chatanantavet, P., Lamb, M. P., & Nittrouer, J. A. (2012). Backwater controls on avulsion location of deltas. *Geophysical Research Letters*, *39*, L01402. https://doi.org/10.1029/2011GL050197

Crosato, A., & Saleh, M. S. (2011). Numerical study on the effects of floodplain vegetation on river planform style. *Earth Surface Processes and Landforms*, *36*, 711–720.

Cyples, N. N. (2019). Proximal braided-river morphodynamics reconstructed through ground-penetrating radar and multi-temporal remote sensing: Kicking Horse River, British Columbia, Canada. A thesis submitted in partial fulfillment of the requirements for the degree of Master of Science (MSc) in Geology, The Faculty of Graduate Studies Laurentian University Sudbury, Ontario, Canada, (pp. 1–82).

Cyples, N. N., Ielpi, A., & Dirszowsky, R. W. (2020). Planform and stratigraphic signature of proximal braided streams: Remote sensing and ground-penetrating-radar analysis of the Kicking Horse River, Canadian Rocky mountains. *Journal of Sedimentary Research*, *90*, 131–149.

Duda, T., & Borówka, R. K. (2007). Zmiany w krajobrazie doliny dolnej Odry na te rozwoju paleogeograficznego regionu (summary in English: Changes in the lower Odra valley landscape in the context of paleogeographic development of the region). *Prace Komisji Krajobrazu Kulturowego*, *7*, 210–218.

Durkin, P. R., Hubbard, S. M., Holbrook, J., & Boyd, R. (2018). Evolution of fluvial meander belt deposits and implications for the completeness of the stratigraphic record. *GSA Bulletin*, *130*, 721–739.

Egozi, R., & Ashmore, P. (2008). Defining and measuring braiding intensity. *Earth Surface Processes and Landforms*, *33*, 2121–2138.

Entwistle, N., Heritage, G., & Milan, D. (2018). Food energy dissipation in anabranching channels. *River Research and Applications*, *34*, 709–720.

Feeney, C. J., Chiverrell, R. C., Smith, H. G., Hooke, J. M., & Cooper, J. R. (2020). Modelling the decadal dynamics of reach-scale river channel evolution and floodplain turnover in CAESAR-Lisflood. *Earth Surface Processes and Landforms*, *45*, 1273–1291.

Ferguson, R. (1987). Hydraulic and sedimentary controls of channel pattern. In K.Richards (Ed.) *River channels: Environment and process* (pp. 129–158). Institute of British Geographers, Special Publication 18, Blackwell, Oxford.

Fielding, C. R., Alexander, J., & Allen, J. P. (2018). The role of discharge variability in the formation and preservation of alluvial sediment bodies. *Sedimentary Geology*, *365*, 1–20.

Friend, P. F., & Sinha, R. (1993). Braiding and meandering parameters. In J. L. Best, & C. S. Bristow (Eds.), *Braided rivers* (Vol. 75, pp. 105–111). Geological Society Special Publication.

Gábris, G., & Nádor, A. (2007). Long-term fluvial archives in Hungary: Response of the Danube and Tisza rivers to tectonic movements and climatic changes during the quaternary: A review and new synthesis. *Quaternary Science Reviews*, *26*, 2757–2782.

Gałka, M., Feurdean, A., Hutchinson, S., Milecka, K., Tanţău, I., & Apolinarska, K. (2018). Response of a spring-fed fen ecosystem in central-eastern Europe (NW Romania) to climate changes during the last 4000 years: A high-resolution multi-proxy reconstruction. *Palaeogeography, Palaeoclimatology, Palaeoecology*, *504*, 170–185.

Ganti, V., Hajek, E. A., Leary, K., Straub, K. M., & Paola, C. (2020). Morphodynamic hierarchy and the fabric of the sedimentary record. *Geophysical Research Letters*, *47*, e2020GL087921. https://doi.org/10.1029/2020GL087921

Gibling, M. R. (2006). Width and thickness of fluvial channel bodies and valley fills in geological record: A literature compilation and classification. *Journal of Sedimentary Research*, *76*, 731–770.

Gibling, M. R., Nanson, G. C., & Maroulis, J. C. (1998). Anastomosing river sedimentation in the channel Country of Central Australia. *Sedimentology*, *45*, 595–619.

Gonera, P., & Kozarski, S. (1987). River channel changes and rough palaeodischarge estimates for the Warta River, west-central Poland. *Geografiska Annaler – Series A: Physical Geography*, *69A*, 163–171.

Gradziński, R., Baryła, J., Danowski, W., Doktor, M., Gmur, D., Gradziński, M., et al. (2000). Anastomosing system of the upper Narew River, NE Poland. *Annales Societatis Geologorum Poloniae*, *70*, 219–229.

Gradziński, R., Baryła, J., Doktor, M., Gmur, D., Gradziński, M., & Kędzior, A. (2003). Vegetation-controlled modern anastomosing system of the upper Narew River (NE Poland) and its sediments. *Sedimentary Geology*, *157*, 253–276.

Hildebrandt-Radke, I. (2013). Pradziejowa i wczesnohistoryczna antropopresja i jej zapis w środowisku przyrodniczym na przykładzie regionu środkowej Obry (Wielkopolska) (in Polish). Seria: Studia I Prace Z Geografii I Geologii, 30, Wydawnictwo Naukowe Bogucki, pp. 158.

Hooke, J. M. (1995). River channel adjustment to meander cutoffs on the River Bollin and River Dane, northwest England. *Geomorphology*, *14*, 235–253.

Hooke, J. M. (2004). Cutoffs galore! Occurrence and causes of multiple cutoffs on a meandering rivers. *Geomorphology*, *61*, 225–238.

Hooke, J. M. (2007). Spatial variability, mechanisms and propagation of change in an active meandering channel. *Geomorphology*, *84*, 277–296.

Jansen, J. D., Nanson, G. C., Cohen, T. J., Fujioka, T., & Fabel, D. (2013). Lowland river responses to intraplate tectonism and climate forcing quantified with luminescence and cosmogenic ^{10}Be. *Earth and Planetary Science Letters*, *366*, 49–58.

Jervey, M. T. (1988). Quantitative geological modeling of siliciclastic rock sequences and their seismic expression. In C. K. Wilgus, B. S. Hastings, C. G. S. C. Kendall, H. W. Posamentier, C. A. Ross, & J. C. van Wagoner (Eds.), *Sea-level changes: An integrated approach* (Vol. 42, pp. 47–69). Spec. Publ. Soc. Econ. Paleont. Miner.

Kaiser, K., Lorenz, S., Germer, S., Juschus, O., Küster, O., & Libra, J. (2012). Late Quaternary evolution of rivers, lakes and peatlands in northeast Germany reflecting past climatic and human impact – An overview. *Quaternary Science Journal*, *61*, 103–132.

Kalicki, T. (1991). The evolution of the Vistula river valley between Cracow and Niepołomice in late Vistulian and Holocene times. In: In L. Starkel (Ed.), *The evolution of the Vistula River valley during the last 15000 year, IV. Geographical Studies, Special Issue* 6, 11–37.

Kasse, C., Bohncke, S. J. P., Vandenberghe, J., & Gábris, G. (2010). Fluvial style changes during the last glacial-interglacial transition in the middle Tisza valley (Hungary). *Proceedings of the Geologists Association*, *121*, 180–194.

Kleinhans, M. G., de Haas, T., Lavooi, E., & Makaske, B. (2012). Evaluating competing hypotheses for the origin and dynamic of river anastomosis. *Earth Surface Processes and Landforms*, *37*, 1337–1351.

Kleinhans, M. G., & van den Berg, J. H. (2011). River channel and bar patterns explained and predicted by an empirical method and a physics-based methods. *Earth Surface Processes and Landforms*, *36*, 721–738.

Kołaczek, P., Płóciennik, M., Gałka, M., Apolinarska, K., Tosik, K., Gąsiorowski, M., et al. (2018). Persist or take advantage of global warming: A development of early Holocene riparian forest and oxbow lake ecosystems in central Europe. *Quaternary Science Reviews*, *200*, 191–211.

Lamentowicz, M., Gałka, M., Lamentowicz, Ł., Obremska, M., Kühl, N., Lücke, A., et al. (2015). Reconstructing climate change and ombrotrophic bog development during the last 4000 years in northern Poland using biotic proxies, stable isotopes and trait-based approach. *Palaeogeography, Palaeoclimatology, Palaeoecology*, *418*, 261–277.

Latrubesse, E. M. (2015). Large rivers, mega fans and other Quaternary avulsive fluvial systems: A potential "who is who" in the geological record. *Earth-Science Reviews*, *146*, 1–30.

Latrubesse, E. M., Cozzuol, M., da Silva-Caminha, S. A. F., Rigsby, C. A., Absy, M. L., & Jaramilo, C. (2010). The late Miocene palaeogeography of the Amazon basin and the evolution of the Amazon River system. *Earth-Science Reviews*, *99*, 99–124.

Leopold, L., & Wolman, M. G. (1957). River channel patterns: Braided, meandering and straight. Geological Survey professional paper, 282-B, 1–70.

Lóczy, D., & Dezső, J. (2013). Groundwater flooding hazard in river valleys of hill regions: Examples of the Kapos river, Southwest-Hungary. *Hungarian Geographical Bulletin*, *62*, 157–174.

Luchi, R., Hooke, J. M., Zolezzi, G., & Bertoldi, W. (2010). Width variations and mid-channel bar inception in meanders: River Bollin (UK). *Geomorphology*, *199*, 1–8.

Lunt, I. A., Bridge, J. S., & Tye, R. S. (2004). A quantitative, three-dimensional model of gravelly braided rivers. *Sedimentology*, *51*, 377–414.

Magyari, E. K., Chapman, J., Fairbairn, A. S., Francis, M., & de Guzman, M. (2012). Neolithic human impact on the landscapers of northeast Hungary inferred from pollen and settlement records. *Vegetation History and Archaeobotany*, *21*, 279–302. https://doi.org/10.1007/s00334-012-0350-6

Makaske, B. (2001). Anastomosing rivers: A review of their classification, origin and sedimentary products. *Earth-Science Reviews*, *53*, 149–196.

Makaske, B., Lavooi, E., de Haas, T., Kleinhans, M. G., & Smith, D. G. (2017). Upstream control of river anastomosis by sediment overloading, the upper Columbia River, British Columbia, Canada. *Sedimentology*, *64*, 1488–1510.

Makaske, B., Smith, D. G., & Berendsen, H. J. A. (2002). Avulsions, channel evolution and floodplain sedimentation rates of the anastomosing upper Columbia River, British Columbia, Canada. *Sedimentology*, *49*, 1049–1071.

Marcinkowski, P., Kiczko, A., & Okruszko, T. (2018). Model-based analysis of macrophytes role in the flow distribution in the anastomosing river system. *Water*, *10*, 953. https://doi.org/10.3390/w10070953

Marks, L. (2012). Timing of the late Vistulian (Weichselian) glacial phases in Poland. *Quaternary Science Reviews*, *44*, 81–88.

Menting, F., & Meijles, E. W. (2019). Local factors determining spatially heterogeneous channel migration in a low-energy stream. *Water*, *11*, 2149. https://doi.org/10.3390/w11102149

Miall, A. D. (1985). Architectural-element analysis: A new method of facies analysis applied to fluvial deposits. *Earth-Science Reviews*, *22*, 261–308.

Morisawa, M. (1985). *Rivers: Form and processes* (p. 222). Longman

Mosley, P. M. (1981). Semi-determinate geometry of river channels, South Island, New Zealand. *Earth Surface Processes and Landforms*, *6*, 127–137.

Neretin, L. N., Volkov, I. I., Rozanov, A. G., Demidova, & Falina, A. (2006). Biogeochemistry of the Black Sea anoxic zone with a reference to sulphur cycle. In L. N. Neretin (Ed.), *Past and present water column anoxia* (pp. 69–104). Springer.

Nicolas, A. P., Sambrook Smith, G. H., Amsler, M., Ashworth, P. J., Best, J. L., Hardy, R. J., et al. (2016). The role of discharge variability in determining alluvial stratigraphy. *Geology*, *44*, 3–6.

Nowaczinski, E., Schukraft, G., Keller, C., Hecht, S., & Eitel, B. (2015). Fluvial dynamics of the Žitava River, SW Slovakia, during the last 45 ka BP and their influence on Early Bronze Age human occupation. *Quaternary International*, *370*, 113–126.

Panin, A., Borisova, O., Konstantinov, E., Belyayev, Y., Eremenko, E., Zakharov, A., et al. (2020). The late quaternary evolution of the upper reaches of fluvial systems in the Southern East European Plain. *Quaternary*, *3*, 31. https://doi.org/10.3390/quat3040031

Paola, C., Ganti, C., Mohrig, D., Runkel, A. C., & Straub, K. M. (2018). Time not our time: Physical controls on the preservation and measurement of geologic time. *Annual Review of Earth and Planetary Sciences*, *46*, 409–428.

Pécsi, M. (1959). *A magyarországi Duna-völgy kialakulása és felszínalaktana (in Hungarian)* (p. 346). Akadémiai Kiadó.

Roggenkamp, T., & Herget, J. (2000). Middle and lower Rhine in Roman times: A reconstruction of hydrological data based on historical sources. *Environmental Earth Sciences*, *75*, 1100, https://doi.org/10.1007/s12665-016-5909-0

Rotnicki, K. (1991). *Retrodiction of paleodischarges of meandering and sinuous alluvial rivers and its paleoclimatic implications*. In L. Starkel, K. J. Gregory, & J. B. Thornes (Eds.), Temperate paleohydrology (pp. 431–471). Chichester, Wiley.

Rotnicki, K., & Młynarczyk, Z. (1989). Późnovistuliańskie i holoceńskie formy i osady korytowe środkowej Prosny i ich paleohydrologiczna interpretacja (summary in English: Late Vistulian and Holocene channel forms and deposits of the middle Prosna river and their palaeohydrological interpretation). *Seria Geografia*, *43*, 1–76.

Sambrook Smith, G. H., Ashworth, P. J., Best, J. L., Woodward, J., & Simpson, C. J. (2006). The sedimentology and alluvial architecture of the sandy braided South Saskatchewan River, Canada. *Sedimentology*, *53*, 413–434.

Shanley, K. W., & McCabe, P. J. (1991). Predicting facies architecture through sequence stratigraphy: An example from the Kaiparowits plateau. *Utah Geology*, *19*, 742–745.

Słowik, M. (2011). Reconstructing migration phases of meandering channels by means of ground-penetrating radar (GPR): The case of the Obra River, Poland. *Journal of Soils and Sediments*, *11*, 1262–1278.

Słowik, M. (2013). Transformation of a lowland River from a meandering and multi-channel pattern into an artificial canal: Retracing a path of river channel changes (the middle Obra River, W Poland). *Regional Environmental Change*, *13*, 1287–1299.

Słowik, M. (2014). Reconstruction of anastomosing river course by means of geophysical and remote sensing surveys (the Middle Obra Valley, W Poland). *Geografiska Annaler – Series A: Physical Geography*, *96*, 195–216.

Słowik, M. (2016a). The influence of meander bend evolution on the formation of multiple cutoffs: Findings inferred from floodplain architecture and bend geometry. *Earth Surface Processes and Landforms*, *41*, 626–641.

Słowik, M. (2016b). Sedimentary record of point bar formation in laterally migrating anabranching and single-channel meandering rivers (the Obra Valley, Poland). *Zeitschrift für Geomorphologie*, *60*, 259–279.

Słowik, M. (2018). The formation of an anabranching planform in a sandy floodplain by increased flows and sediment load. *Earth Surface Processes and Landforms*, *43*, 623–638.

Słowik, M., Dezső, J., Kovács, J., & Gałka, M. (2020). The formation of low-energy meanders in loess landscapes (Transdanubia, Central Europe). *Global and Planetary Change*, *184*, 103071. https://doi.org/10.1016/j.gloplacha.2019.103071

Słowik, M., Dezső, J., Kovács, J., Gałka, M., & Sipos, G. (2021). Phases of fluvial activity in loess landscapes: Findings from the Sió Valley (Transdanubia, Central Europe). *Catena*, *198*, 105053. https://doi.org/10.1016/j.catena.2020.105054

Słowik, M., Gałka, M., & Marciniak, A. (2020). The evolution and disappearance of "false delta" multi-channel systems in postglacial areas (Central Europe). *Global and Planetary Change*, *184*, 103044. https://doi.org/10.1016/j.gloplacha.2019.103044

Sobkowiak-Tabaka, I., Pawłowski, D., Milecka, K., Kubiak-Martens, L., Kostecki, R., Janczak-Kostecka, et al. (2019). Multi-proxy records of Mesolithic activity in the Lubuskie Lakeland (western Poland). *Vegetation History and Archaeobotany*. https://doi.org/10.1007/s00334-019-00752-3

Starkel, L. (2001). *Historia doliny Wisły od ostatniego zlodowacenia do dziś (summary in English: Evolution of the Vistula River valley since the last glaciation till present). Polska Akademia Nauk, Instytut Geografii i Przestrzennego Zagospodarowania im* (p. 263). Stanisława Leszczyckiego.

Starkel, L., Kalicki, T., Krąpiec, M., Soja, R., Gębica, P., & Czyżowska, E. (1996). Evolution of the Vistula River valley during the last 15000 years (Vol. *9*, pp. 1–158). *Geographical Studies, Special Issue*.

Starkel, L., Soja, R., & Michczyńska, D. J. (2006). Past hydrological events reflected in Holocene history of Polish rivers. *Catena*, *66*, 24–33.

Toonen, W. H. J., Kleinhans, M. G., & Cohen, K. M. (2012). Sedimentary architecture of abandoned channel fills. *Earth Surface Processes and Landforms*, *37*, 459–472.

Tóth, O., Sipos, G., Kiss, T., & Bartyik, T. (2017). Dating the Holocene incision of the Danube in southwestern Hungary. *Journal of Environmental Geography*, *10*, 53–59.

Turkowska, K., Forysiak, J., Petera, J., & Miotk-Szpiganowicz, G. (2004). A Warta River system during the Younger Dryas in the Koło Basin (middle Poland). *Quaestiones Geographicae*, *23*, 83–107.

Uścinowicz, S. (2004). *Rapid sea level changes in the southern Baltic during late glacial and early Holocene* (Vol. *11*, pp. 9–18). Polish Geological Institute Special Papers.

van de Lageweg, W. I., van Dijk, W. M., Box, D., & Kleinhans, M. G. (2016). Archimetrics: A quantitative tool to predict three-dimensional meander bend heterogeneity. *Depositional Record*, *2*, 22–46.

van den Berg, J. H. (1995). Prediction of alluvial channel pattern of perennial rivers. *Geomorphology*, *12*, 259–279.

Vandenberghe, J., Kasse, C., Popov, D., Markovic, S. B., Vandenberghe, D., & Gábris, G. (2018). Specifying the external impact on fluvial lowland evolution: The last glacial Tisza (Tisa) catchment in Hungary and Serbia. *Quaternary v*, *1*, 14. https://doi.org/10.3390/quat1020014

van Dijk, W. M., van de Lageweg, W. I., & Kleinhans, M. G. (2012). Experimental meandering river with chute cutoffs. *Journal of Geophysical Research*, *117*, F03023. https://doi.org/10.1029/2011JF002314